Sustainable Energy, Grids and Networks 44 (2025) 101993

Contents lists available at ScienceDirect

Sustainable Energy, Grids and Networks

journal homepage: www.elsevier.com/locate/segan

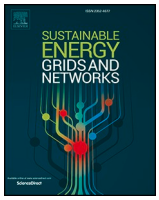

Improving transmission line resilience against hurricane-induced cascading outages by preventing maloperation of vulnerable zone 3 distance relays

Seyyed Alireza Modaberi [a], Sajjad Tohidi [a,*], Saeid Ghassem Zadeh [a], Tohid Ghanizadeh Bolandi [b]

[a] Faculty of Electrical & Computer Engineering, University of Tabriz, Tabriz, Iran
[b] Faculty of Electrical & Computer Engineering, Urmia University, Urmia, Iran

ARTICLE INFO

Keywords:
Resilience
Transmission network
Cascading outage
Hurricane
Relay vulnerability
Load encroachment

ABSTRACT

High-impact, low-probability events such as hurricanes can severely affect transmission networks, causing cascading outages of transmission lines and leading to power system instability. When transmission lines are disconnected, power flow transfer phenomena may occur, resulting in the redistribution of power to healthy lines and potentially causing overloading. This condition often triggers load encroachment into Zone 3 of distance relays on unaffected lines, leading to their unintended operation. Such maloperation can propagate cascading outages and accelerate system instability. This paper aims to enhance the resilience of transmission networks against cascading outages induced by hurricanes. The primary objective is to identify and monitor the performance of vulnerable Zone 3 distance relays to prevent their contribution to the spread of outages. By mitigating relay maloperations, the number of line outages due to incorrect tripping is reduced. A new hurricane model based on the Rankine vortex is proposed to improve the prediction of transmission line outages associated with hurricanes. The model estimates wind speeds over time, tracks the spatial and temporal evolution of hurricanes, and enables more accurate modeling of hurricane-induced cascading outages. Additionally, two novel indices are introduced: one for evaluating the vulnerability of Zone 3 distance relays and another for distinguishing between three-phase symmetrical faults and load encroachment conditions. The proposed methodology is implemented on the 39-bus New England test system. Simulation results confirm the method's effectiveness and efficiency.

1. Introduction

The frequency and severity of extreme weather events have increased significantly in recent years due to climate change [1]. HILP events may lead to massive power outages [2]. Since some consequences of power outages cause heavy damage to society, improving the power system's resilience against natural and man-made disasters is of great importance [3]. Hurricane as a natural event, can affect the sustainability of transmission lines over several hours. Based on the fragility curve of transmission lines, the vulnerabilities of towers and equipment depend on wind speed. Therefore, a more accurate estimation of the wind speed imposed by hurricanes on network components can yield a more precise assessment [4]. On the other hand, line outages caused by hurricanes can lead to overloading of the remaining healthy lines in the network, causing LE into Zone 3 of the network's distance relays [5]. Undesired operation of vulnerable Zone 3 distance relays can spread cascading outages and accelerate network instability. Therefore, improving the resilience of the transmission network against cascading outages caused by storms—by preventing the maloperation of critical Zone 3 distance relays—is an important research area that has received less attention.

The impacts of hurricanes on the infrastructure of power transmission networks are investigated in [6–8]. Different hurricane models are used to simulate the event and determine wind speeds at various points within the transmission network. In some cases, the power system is divided into sections, and using recorded historical data, the wind speed for a particular section is assumed to be constant [9]. Other models use mathematical equations to estimate hurricane conditions. Mathematical-based models are also divided into two types: some consider the changing dynamics of hurricanes, while others do not. Models like Batt capture the changing trend of hurricanes [10]. In this model, in addition to wind speed data, air pressure data is also required, which leads to extensive calculations. In contrast, models such as the MRVM do not consider the changing process of a hurricane, making them easier to use. Hence, an easy-to-use hurricane model that can

* Corresponding author.
E-mail address: stohidi@tabrizu.ac.ir (S. Tohidi).

https://doi.org/10.1016/j.segan.2025.101993
Received 17 May 2025; Received in revised form 29 August 2025; Accepted 27 September 2025
Available online 29 September 2025

Nomenclature

Parameters & Variables

$F(t_1)$	Power System Performance before the Event
$F(t_2)$	Performance of the Damaged System
r	Radial Distance from the Center of the Hurricane
R_{max}	Radius at which the Maximum Wind Speed Occurs
V_{max}	Maximum Wind Speed at R_{max}
X	Shape Parameter
V_{enter}	Wind Speed at the Entrance of the Land
V_{exit}	Wind Speed at the Exit of the Land
N	Number of Concentric Circles
$V_{step,i}$	Wind Speeds at Steps I
$V_{step,i-1}$	Wind Speeds at Steps I −1
$P_T(w)$	Failure Probabilities of an Individual Tower
$P_{Eq}(w)$	Failure Probabilities of an Individual Equipment
$w_{critical}$	Critical Wind Speed
$w_{collapse}$	Wind Speed at which the Line Collapses
P[tower Failure]	Failure Probabilities of the Line Towers
P[Equipment Failure]	Failure Probabilities of the Line Equipment
P_{TN}	Failure Probabilities of the N^{th} Tower
P_{EqN}	Failure Probabilities of the N^{th} Equipment
FP	Failure Probability
FT	Failure Time
$P_L(w)$	Line Failure Probability at Wind Speed w
Ti	I-Th Step of Failure Time Calculation
Pj	J-Th Step of Failure Probability Calculation
Ind_i	I^{th} Concentric Circle
k	Mean of Ind_{i1} and Ind_{i2}
C_k	Position of the Center of the K-Th Circle
C_{enter}	Landfall Point of the Hurricane
V_{moving}	Hurricane's Forward Movement Speed
CFC	Cascading Failure Chain
L_{fn}	Removed Line Due to Hurricane
fn	Total Number of Removed Lines
$LVPI$	Line Vulnerability Probability Index
Z_{seen}	Impedance Seen by the Distance Relay
$Z_{set,\ zone\ 3,\ ij}$	Setting Impedance for Zone 3 of the Distance Relay
Z_{ij}	Impedance of the Protected Line
RM	Relay Margin
RM_e	Relay Margin under Event Conditions
RM_o	Relay Margin in Normal Network Operation Mode
$\boldsymbol{f}$	a Failure Scenario of Transmission Lines Caused by A Hurricane
$\boldsymbol{Y_i}$	I^{th} Distance Relay
$\boldsymbol{NG}$	Number of Groups
m	Number of Group's Members
S	Total Number of Hurricane Scenarios
VP_R	Vulnerability Probability of the Relay
OP_{gi}	Occurrence Probability of the I^{th} Group
FP_{Ri}	Failure Probability of the Relays In the Corresponding Group
Z_f	Fault Impedance
ΔU	Positive-Sequence Fault Component Voltage Phasors
ΔI	Positive-Sequence Fault Component Current Phasors
ΔS	Phasor Quantities of Superimposed Component Complex Power
P-mo	Maloperation Probability of the Relay

Abbreviations

HILP	High-Impact, Low-Probability
MRVM	Modified Rankine Vortex Model
PMU	Phasor Measurement Unit
LE	Load Encroachment
MI	Monitoring Index
PSIA	Positive-Sequence Impedance Angle
SSC	Step of Speed Change
VL	Vulnerability Level
VI	Vulnerability Index
SCCP	Superimposed Component Complex Power
DPAISCP	Differential Phase Angle of Integrated Superimposed Complex Power

simulate the hurricane's changing process and estimate wind speeds on components at various times is still required. A combination of the Batt and MRVM models might present a simple yet effective model by considering the hurricane's changing dynamics.

The vulnerability assessment of transmission networks should be conducted as a crucial stage of resilience evaluation to identify critical components. A HILP disaster triggers faults that can decrease the stability of a power system. For instance, during a hurricane, several transmission lines may be disconnected simultaneously, leading to changes in the network's power flow patterns. This causes power flow to transfer from the damaged lines to the healthy ones, imposing overload on them. Consequently, hurricanes not only cause line disconnections but also alter the power flow patterns within the network. PMUs can be used as an effective approach to monitor network conditions under such stressed scenarios [11]. These units provide real-time data on the lines, which can be used to implement appropriate corrective and recovery measures to enhance network resilience [12]. During a hurricane, components of a transmission network may fail sequentially, depending on wind intensity and the hurricane's path. Numerous studies have investigated the effects of hurricanes on various sectors of the power system. In some, it is assumed that transformers, cables, and power plants remain undamaged by extreme weather events [13,14]. For example, [13] uses HAZUS software to identify and classify wind speeds in areas affected by hurricane into three categories: high impact, medium impact, and low impact. Based on this classification, the vulnerability of different parts of the power system—including transmission lines, substations, and wind farms—is assessed to provide planning schemes aimed at increasing resilience. In [15], the vulnerability of a transmission network under a hurricane is evaluated by simulating an MRVM-based hurricane event on a 118-bus network. This study models the fault chain of lines caused by wind and overload without considering the sequence of line outages. Reference [16] uses Monte Carlo simulation to generate hurricane winds for transmission network planning, taking into account the effects of battery energy storage and wind farms. In [17], an attacker-defender optimization model is developed for vulnerability assessment and resilience-oriented planning of transmission networks. Here, attackers represent natural phenomena causing severe system damage, while defenders represent actions to minimize system vulnerabilities. Reference [18] proposes a model for resilience-oriented transmission expansion planning that considers optimal transmission switching during hurricane events. This study models component vulnerability uncertainty by creating a hurricane-related uncertainty set. In [19], the authors propose an aggregated vulnerability assessment framework for the transmission lines, combining operational and hurricane-induced outages. A weather-based failure rate index is developed using simulated hurricane scenarios. This is integrated with standard performance indices in a fuzzy inference system to produce an aggregated vulnerability index. The method effectively ranks the line vulnerability and supports the resilience planning. Moreover, in [20], a resilience-oriented transmission expansion planning approach that accounts for hurricane-induced impacts by identifying vulnerable transmission lines

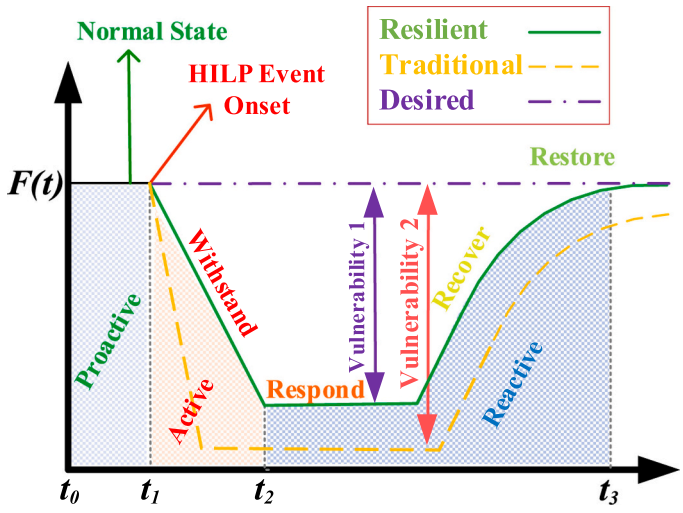

Fig. 1. resilience curve of power system [1].

and implementing targeted system hardening strategies is presented. The proposed optimization model incorporates failure probabilities—derived from line exposure and hardening costs—into the planning process. Validated using a real-world power grid and historical hurricane data, the framework demonstrates its effectiveness in reducing expected outage costs and enhancing the system resilience through strategic line reinforcements.

While existing studies have examined the impact of hurricanes on transmission networks, the sequence of line outages caused by such event has not been sufficiently evaluated.

The aim of Zone 3 protection in the distance relay is to provide a remote backup protection method for all transmission lines connected to the remote end. To achieve this, the reach of the backup protection zone is set to cover the longest line connected to the remote bus. This may cause the impedance seen by the relay to fall within its operating zone under stressed system conditions, such as overload. As a result, undesired operation of Zone 3 in the distance relay may occur, potentially leading to cascading outages in the power system [21]. Cascading outages of transmission lines are a significant concern in power systems [22]. The primary cause of rare and costly blackouts in transmission networks is cascading failure. Under stressed conditions, maloperation of Zone 3 distance relays can trigger cascading outages due to LE, which has been reported as a significant factor contributing to disruptive blackouts [23]. Various methods have been proposed to improve the performance of vulnerable Zone 3 distance relays [24]. Some are based on concentric characteristics, such as the method proposed in [25], which measures the time it takes for the impedance trajectory to cross concentric boundaries. If this time exceeds a certain threshold, the condition is classified as non-fault. However, this method cannot detect symmetrical faults when the relay is blocked under non-fault conditions such as power swings. Among the proposed solutions for distinguishing LE, using fault superimposed components has been reported as an effective method to differentiate symmetrical three-phase faults from [26]. The contribution of vulnerable Zone 3 distance relays to the spread of hurricane-induced cascading outages has not yet been investigated.

Recently, fault superimposed component-based protection methods have been presented as powerful techniques for modern distribution and transmission networks [27–33]. In [27], a novel index called the differential phase angle of the superimposed complex power is proposed as a resilient approach for protecting active AC microgrids. This method can quickly and accurately detect various types of faults in different locations, whether in grid-connected or islanded microgrid modes. In [28], by equipping digital critical distance relays with Global Positioning System, a novel approach for vulnerability assessment of Zone 3 distance relays is presented. A new MI is proposed for real-time and regional monitoring of backup protections. However, no reliable method has yet been provided for detecting and ranking vulnerable distance relays. In [29], a new technique to extract fault features based on the superimposed components of Lissajous patterns is introduced to estimate fault type and location on transmission lines. In [30], a superimposed component-based protection scheme for multi-terminal transmission lines is proposed, using phaselet transform to estimate phasors in less than one full cycle. This scheme demonstrates reliable performance during transients such as current transformer saturation and capacitor bank switching. In [31], a differential protection scheme utilizing fundamental frequency superimposed current phasors is proposed for AC microgrid feeders, where phasors are derived using dq components instead of traditional Fourier algorithms. In [32], superimposed positive-sequence real power is used to distinguish internal faults from external ones in microgrids; however, its effectiveness in detecting symmetrical faults during overloads has not been evaluated. Besides, a local protection scheme for the distance relay Zone 3 that utilizes three novel indices—an out-of-step detection index, a PSIA index, and a superimposed PSIA index—is proposed in [34] to distinguish between short-circuit faults and stressed system conditions. Theoretical formulations underpin the determination of index thresholds, which are then validated through comprehensive static and dynamic analyses. Simulation results confirm the approach's effectiveness under diverse stressed scenarios, including inverter-based resources, while maintaining cost-efficiency by eliminating the requirement for synchrophasor measurements or communication infrastructure. From the review of the above-mentioned articles, it can be concluded that fault superimposed components are an effective approach for monitoring the operation of critical relays involved in the propagation of line outages caused by hurricanes.

The main aim of this study is to evaluate the vulnerability of the transmission network to hurricanes and to present a reliable approach for improving transmission line resilience against hurricane-induced cascading outages by preventing the maloperation of critical Zone 3 distance relays. A review of the literature reveals that the resilience of transmission networks—specifically by preventing vulnerable relays from increasing the number of line outages caused by hurricanes—has not been sufficiently investigated. In this study, as a first step, a new hurricane model is proposed for accurate modeling of transmission line disconnections caused by hurricanes. Next, a novel approach is introduced to identify Zone 3 distance relays that are vulnerable and have a high likelihood of participation in hurricane-induced outages. Finally, a MI based on superimposed components is proposed to monitor the performance of vulnerable relay(s). In summary, the main contributions of this paper are as follows:

- Proposing an accurate hurricane model based on the Rankine vortex model.
- Identifying vulnerable lines and their outage sequences due to hurricanes.
- Determining vulnerable relays affected by hurricane-induced line outages.
- Providing a new MI for monitoring the critical distance relays to distinguish LE event from symmetrical faults.

The rest of the paper is organized as follows. Section 2 provides an overview of power system resilience. Section 3 presents the proposed hurricane model. Section 4 discusses the resilience assessment of the transmission network and introduces a new algorithm for assessing line vulnerability under hurricane events. Section 5 focuses on the vulnerability assessment of Zone 3 distance relays during hurricanes, proposing a new VI for identifying critical Zone 3 relays, along with two algorithms to determine relay VLs in typical scenarios. Section 6 introduces a detection scheme, featuring a novel index to distinguish symmetrical faults from LE. The proposed methods are validated in Section 7 through performance evaluation on the IEEE 39-bus New England test system. In

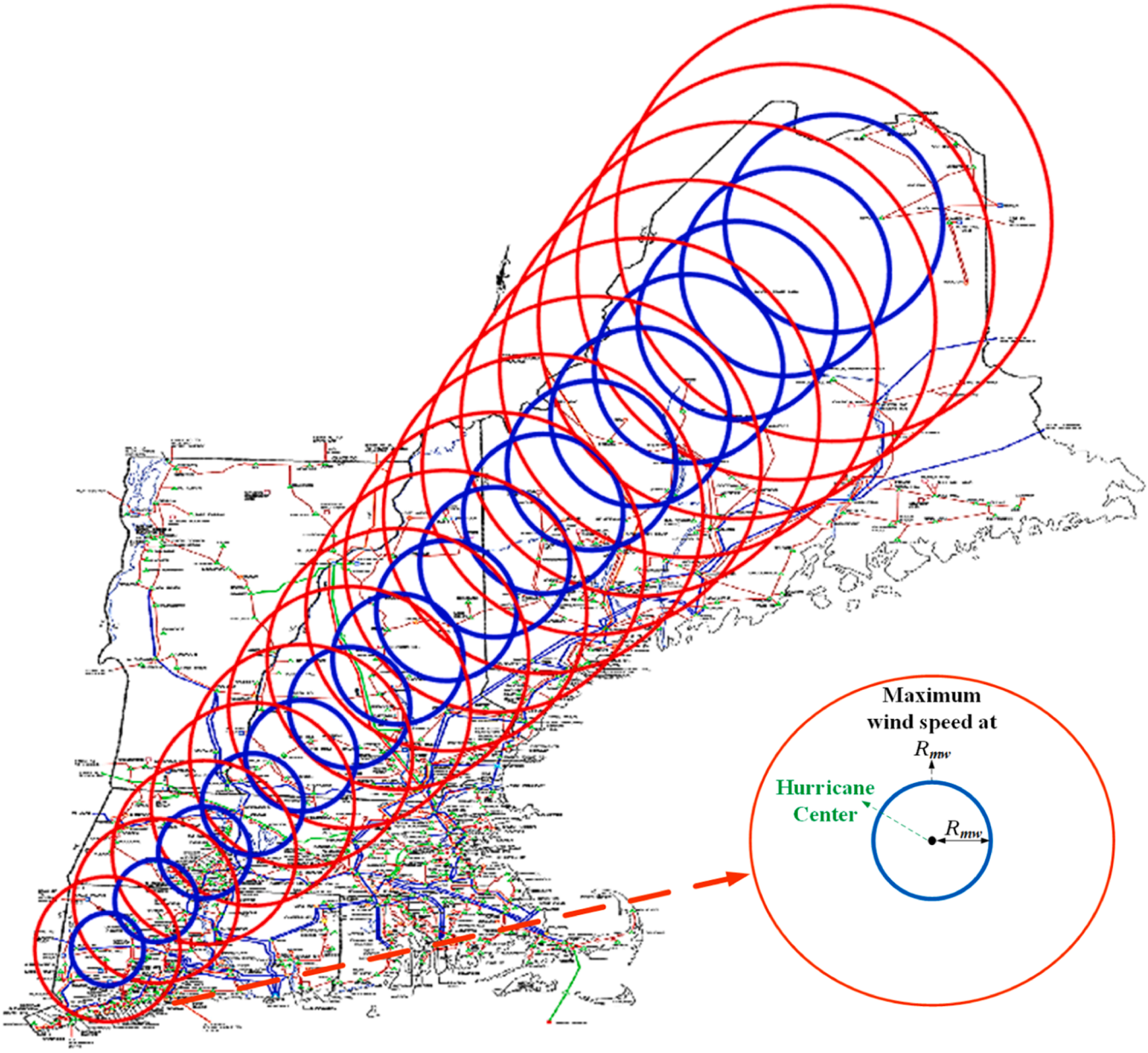

Fig. 2. Proposed modified Rankine vortex model in the New England map.

Section 8, challenges and related issues are discussed. Finally, conclusions are drawn in Section 9.

2. Power system resilience

The aim of resilience studies is to investigate the impact of HILP disasters on the system to identify vulnerable sectors and propose preventive, corrective, and restorative measures to improve system resilience at three stages: before, during, and after an event [35]. Severe HILP events can cause significant damage to power system equipment and infrastructure. These destructive occurrences can be categorized into two groups: (i) man-made events and (ii) natural disasters [36]. A review of the frequency of extreme weather events shows an increase in the number of hurricanes in recent years [37]. Since power systems cover wide geographical areas, many of their components are either directly exposed to natural disasters or indirectly affected by external conditions. Consequently, power system resilience has received increasing attention due to the rising frequency of extreme events.

As illustrated in Fig. 1, actions to improve power system resilience can be divided into three levels based on the duration of the extreme event: (i) proactive actions, (ii) active actions, and (iii) reactive actions. According to this framework, the resilience of a power system depends on its ability to withstand disasters and recover rapidly. Increasing the system's coping capability enhances its recovery process. Therefore, if the power system can withstand HILP events by taking appropriate corrective actions, its resilience will be improved. Resilience is the ability of a power grid to withstand severe disturbances and mitigate the damaging impacts of such catastrophes [38]. Based on this definition, this study proposes corrective actions to increase system resilience during the active period, aiming to reduce the damaging effects of hurricanes on the transmission network. Severe hurricanes can lead to outages of transmission lines. According to [39], the maloperation of Zone 3 in vulnerable distance relays significantly contributes to power system disturbances. The North American Electric Reliability Council reports that about 75 % of major disturbances are related to protection system failures [40]. One cause of Zone 3 distance relay maloperation is,

which occurs when power flow transfers from disconnected faulty lines to remaining healthy lines. This event can trigger cascading outages. The magnitude of power flow from disconnected lines may be large enough to cause the apparent impedance seen by vulnerable distance relays to enter their Zone 3.

Without proper monitoring of these relays' performance, incorrect operations may occur, leading to the unintended disconnection of healthy lines and a reduction in power system resilience. Various metrics have been proposed to evaluate power system resilience [41]. One such metric is based on the level of system performance, ***F(t)***, during the withstand phase, denoted as a function of time *t*. In this study, F(t) represents the amount of load supplied by the system at any given moment. The performance loss can be quantified by identifying its maximum deviation from the normal level, as expressed in (1). The system's resilience to the extreme event can be quantified as the reciprocal of its performance loss [42].

$$Loss = \frac{F(t_1) - F(t_2)}{F(t_2)} \tag{1}$$

where $F(t_1)$ represents the power system performance before the event, and $F(t_2)$ represents the performance of the damaged system. This criterion is used in this study to assess the resilience of the power system.

3. Hurricane model

A hurricane is a rotating low-pressure weather system characterized by thunderstorms and sustained wind speeds exceeding 33 m/s [13]. Hurricanes typically form over oceans and move toward land. They are classified into five categories based on wind speed, with minimum wind speeds starting at 33 m/s and maximum speeds exceeding 70 m/s [13]. Generally, a hurricane moves forward at speeds ranging from about 2–12 m/s [43]. In this study, the average forward speed of a hurricane is assumed to be 7 m/s.

The MRVM is a simple and widely used method for estimating wind field data and has been applied in numerous studies [15,17,44]. In this model, concentric circles represent the wind flow in an idealized stationary tropical cyclone. The wind speed is zero at the center, increases rapidly until it reaches its maximum value at a certain radius, and then decreases back to zero as the radius continues to increase. The distribution of wind speed in the modified vortex model is described by (2):

$$V = \begin{cases} V_{\max}\left(\dfrac{r}{R_{mw}}\right)^{X} & \mathrm{r} < \mathrm{R}_{mw} \\ V_{\max}\left(\dfrac{R_{mw}}{r}\right)^{X} & \mathrm{r} \geq \mathrm{R}_{mw} \end{cases} \tag{2}$$

where r represents the radial distance from the center of the hurricane, R_{max} is the radius at which the maximum wind speed occurs, and V_{max} is the maximum wind speed at that radius. The variable X is the shape parameter that adjusts the wind speed distribution and typically ranges between 0.4 and 0.6. In this model, the wind speed is high near landfall but concentrated within a small radius. Conversely, as the storm moves over land, the wind speed decreases while the radius of maximum winds increases [17].

As illustrated in Fig. 2, this study employs an exact hurricane model to predict wind speeds affecting power system components during hurricane events. Using this model, the wind speed at different times and locations can be determined. The input data for the model include the wind speeds at landfall and upon exiting land, the hurricane's forward speed, the distance between concentric circles, the hurricane's maximum radius, and its path. According to Fig. 2, the proposed model consists of several concentric circles arranged in series, with the number of circles depending on the distance between their centers. The hurricane's path is divided into multiple sections corresponding to the number of concentric circles.

The SSCs is calculated by dividing the difference between the wind speeds at the land entrance and exit by the number of concentric circles, as shown in (3). Consequently, the maximum wind speed in each section is equal to the wind speed of the previous section minus the speed change step, calculated by (4). The wind speed calculated for each section is then used as the maximum wind speed in (2).

$$SSC = \frac{V_{enter} - V_{exit}}{N} \tag{3}$$

$$V_{step,i} = V_{step,i-1} - SSC \tag{4}$$

where V_{enter}, V_{exit} and N represent the wind speed at the entrance and exit of the land and the number of concentric circles used in the spatial discretization of the hurricane model, respectively. Also, $V_{step,i}$ and $V_{step,i-1}$ indicate the wind speeds at steps i and i-1, respectively, where $i = 1, 2, \ldots, N$. Increasing the number of overlapping concentric circles improves accuracy but also increases simulation time.

Each concentric circle represents the temporal and spatial position of the hurricane. Since the hurricane's speed and path are known, its location and wind speed at different times can be estimated. Fig. 2 illustrates the proposed hurricane model applied to the New England region. In this figure, the distance between concentric circles is approximately 20 km. Based on this model, transmission line outages caused by hurricanes can be accurately determined, enabling transmission network operators to make proactive decisions. Additionally, the FTs of transmission lines can be estimated based on the hurricane's forward speed. In summary, the main advantages of the proposed model are as follows:

1. Identification of cascading outages of transmission lines due to hurricanes.
2. Determination of wind speeds that cause cascading outages of transmission lines.
3. Estimation of FTs for transmission lines.

It is worth noting that the proposed hurricane model incorporates two key speed parameters: the hurricane's movement speed, set to an average of 7 m/s (within the typical range of 2–12 m/s), and the variable wind speed induced by the hurricane at different locations, ranging from 33 to 70 m/s. For more accurate resilience assessment of the transmission network under hurricane conditions, wind speeds induced by the hurricane are considered starting from 10 m/s. Higher movement speeds are generally associated with increased infrastructure damage. The proposed model estimates the hurricane's location and predicts the FTs of power system components. For accurate modeling, inputs such as movement speed, landfall and departure speeds, and the storm path are required, which are typically obtained from weather stations. Given the inherent uncertainty in hurricane forecasting, collaboration with meteorological agencies is essential for developing reliable planning scenarios [19].

4. Power transmission network resilience assessment

In this section, the resilience of the power transmission network is evaluated. The procedure is based on fragility curves, which represent the failure probabilities of components as a function of wind speed [9]. Initial conditions are applied to the proposed hurricane model to estimate the wind speeds on transmission components during the hurricane's movement path. At each simulation step, the distance between each component and the hurricane center is calculated, with the center of each concentric circle considered as the hurricane center. The wind speed affecting the transmission components is then determined using (2). Using these calculated wind speeds and the corresponding fragility curves, the FP of each component is extracted. The fragility curves used in this paper, derived from the analysis performed with ABAQUS

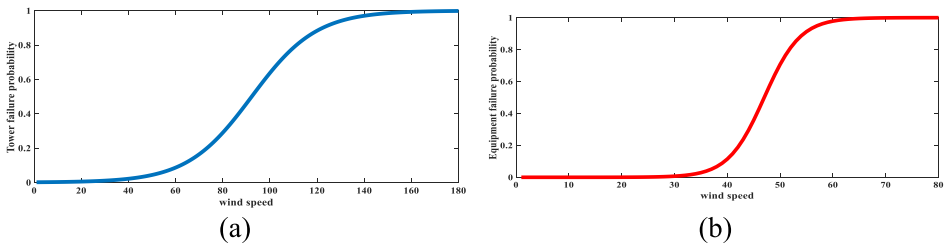

Fig. 3. Fragility curves of (a) tower and, (b) equipment.

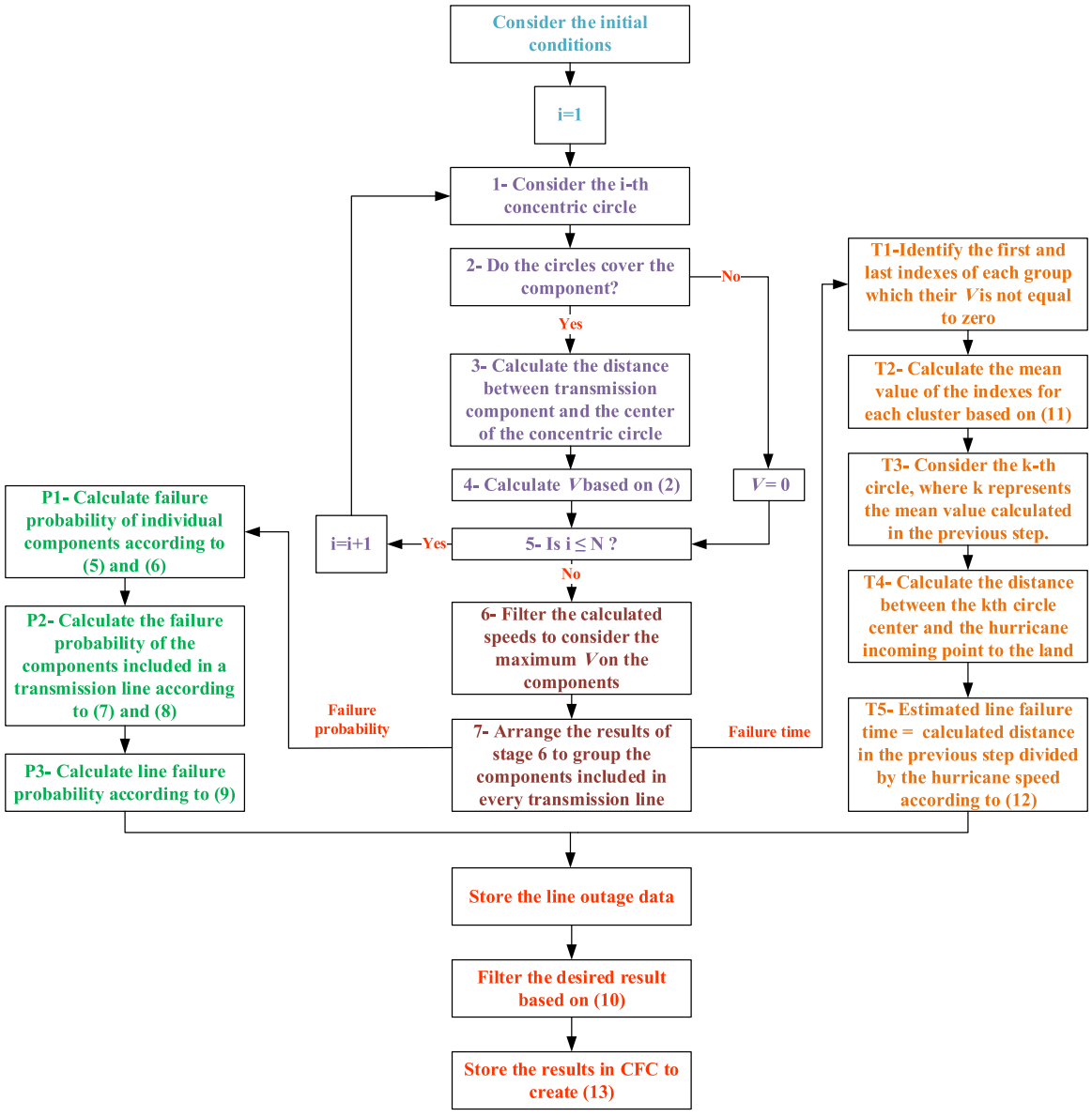

Fig. 4. Resilience assessment of power transmission network against hurricane.

software, are taken from [45]. Fig. 3 illustrates the fragility curves for towers and equipment. Since this study focuses on the resilience of the transmission network, the maximum wind speed experienced by each component is considered.

Therefore, the FP is calculated based on these maximum wind speeds using the fragility curves. The failure probabilities of transmission line components are calculated by using [9], mentioned in (5) and (6):

$$P_T(w) = \begin{cases} 0 if w < w_{critical} \\ P_{T\_hw}(w) if w_{critical} \le w < w_{collapse} \\ 1 if w > w_{collapse} \end{cases} \quad (5)$$

$$P_{Eq}(w) = \begin{cases} 0 if w < w_{critical} \\ P_{Eq\_hw}(w) if w_{critical} \le w < w_{collapse} \\ 1 if w > w_{collapse} \end{cases} \quad (6)$$

where $P_T(w)$ and $P_{Eq}(w)$ represent the failure probabilities of an individual tower and individual equipment (such as shackles), respectively, at a given wind speed w. Additionally, $w_{critical}$ denotes the critical wind speed and, $w_{collapse}$ indicates the wind speed at which the line collapses.

In [45], the values of $w_{critical}$ and $w_{collapse}$ are considered to range between 45 and 150 m/s for towers, while for other network equipment, these values are set at 30 and 60 m/s, respectively. Since a transmission line consists of a series of towers and equipment, their failure probabilities are calculated using (7) and (8).

$$P[TowersFailure] = P_T = 1 - [(1 - P_{T1}(w)) \times (1 - P_{T2}(w)) \times \ldots \times (1 - P_{TN}(w))] \quad (7)$$

$$P[EquipmentFailure] = P_{Eq} = 1 - [(1 - P_{Eq1}(w)) \times (1 - P_{Eq2}(w)) \times \ldots \times (1 - P_{EqM}(w))] \quad (8)$$

where P[*tower Failure*] and P[*Equipment Failure*] are the failure probabilities of the line towers and equipment, respectively. In (7) and (8), P_{TN} and P_{EqN} represent the failure probabilities of the N^{th} tower and equipment of a transmission line, respectively. Finally, the overall line FP is determined by (9).

$$P_L(w) = P_T + P_{Eq} - P_T \times P_{Eq} \quad (9)$$

where $P_L(w)$ represents the line FP at wind speed w. To calculate the FP of the lines, the failure probabilities of individual components are first evaluated using (5) and (6), and then the overall FP of the line is determined using (7) to (9). Here, a component refers to either a tower or a piece of equipment on a transmission line. The resilience evaluation of the power transmission network against a hurricane is carried out using the algorithm shown in Fig. 4. In this approach, each component is assumed to be located at a specific point on an x-y grid. As the hurricane moves along this grid, the distance between the components and the hurricane center changes. According to (2) and (6), the wind speed at any component varies with changes in the hurricane's center location and speed. Thus, in each hurricane scenario, the wind speed affecting each component must be calculated. Since this paper aims to evaluate the resilience of the transmission network, the maximum wind speed experienced by any component across various scenarios is selected. Finally, components belonging to the same line are grouped together to calculate the PF of that transmission line. The above procedure is detailed in steps 1–7 of the proposed algorithm shown in Fig. 4.

In the following, the PF and FT of the components are evaluated based on steps P1–P3 and T1–T5, respectively. In this algorithm, Ti and Pj represent the i-th step of FT calculation and the j-th step of PF calculation, respectively. According to this algorithm, both the PF and FT of each transmission line are determined. These values are then used to identify the cascading outages of transmission lines caused by hurricanes, as explained below.

1. **Calculation of PF**: As mentioned earlier, the PF of lines is extracted using (5)-(9). Then, based on the resilience-oriented planning and operation policies, a failure threshold is established for the lines. Each line whose PF exceed from this threshold is considered as the disconnected line. In Fig. 4, the index of 'threshold' and 'N' indicate the desired threshold value for considering the line outage probability and the number of concentric circles algorithms iterations, respectively. The failed line is determined according to (10):

$$FP = P_L(w) \text{if} P_L(w) > threshold \quad (10)$$

where *FP* is the PF of the line that exceeds the threshold. Therefore, it is considered a candidate for removal due to the hurricane.

2. **Calculation of the FT:** The location of the hurricane determines when a transmission line will fail. The proposed method utilizes the wind speeds obtained at stage 7. In each group, the concentric circles with wind speeds greater than zero represent the zone through which the hurricane is passing. Therefore, the first and last such circles in a group correspond to the entry and exit points of the hurricane along the transmission line. For example, consider a line with 1000 components. If the recorded wind speeds greater than zero start at the 200th component and the last such speed is recorded at the 576th component, then the first and last recorded indices, denoted as Ind_1 and Ind_2, are 200 and 576, respectively. The mean of these indices, i.e., 388, indicates the concentric circle number pointing to the location where the hurricane definitely entered the transmission line. This mean value is represented by 'k' in (11). By calculating the distance between the center of the k-th circle (denoted as C_k in (12)) and the landfall point of the hurricane (denoted as C_{enter} in (12)), and considering the hurricane's forward movement speed (V_{moving}), the FT of the transmission line can be estimated. The FT is formulated by using (12):

$$k = \frac{Ind_2 - Ind_1}{2} \quad (11)$$

$$FT = \frac{C_k - C_{enter}}{V_{moving}} \quad (12)$$

Accordingly, the proposed algorithm evaluates each transmission line's PF and FT based on (10)–(12). Lines that meet the PF condition in (10) are considered candidates for removal from the transmission network. By sorting these candidate lines in ascending order of their FTs, the cascading failure sequence of the lines can be determined. The cascading PF of the lines is then obtained as expressed in (13).

$$CFC = \{L_{f1}, L_{f2}, \ldots, L_{fn}\} \quad (13)$$

where *CFC*, L_{fn}, and *fn* represent the cascading failure chain, the removed line, and the total number of removed lines sorted by their FTs from the smallest to the largest, respectively. In other words, the fault chain could be expressed as: $CFC = \{L_2, L_5, L_{28}, L_3\}$. This means that during the hurricane, the sequence of the line outages follows the order in *CFC*, with the FT of L_2 being the earliest and L_3 being the latest.

The procedure can be repeated for multiple hurricane scenarios by varying the initial conditions of the hurricane. These variations generate different possible scenarios. By utilizing meteorological data for an impending hurricane, the transmission network operator can input this information into the proposed algorithms to make better-informed decisions. After identifying the disconnected lines in each scenario, their contributions are determined. Specifically, the outage probability of a line is defined as the ratio of the number of scenarios in which that line fails to the total number of scenarios simulated. Consequently, the contribution probability of transmission lines across various scenarios—referred to as line vulnerability—is calculated according to the (14).

$$LVPI = \frac{\text{No.ofalineoutagesinvariousscenarios}}{\text{No.ofallthescenarios}} \quad (14)$$

where *LVPI* indicates the line vulnerability probability index.

5. Relay vulnerability assessment

In the previous sections, a novel approach for assessing the resilience of transmission lines against hurricanes was presented. Based on (13), the sequence of line outages caused by a hurricane can be determined. This section focuses on evaluating the vulnerability of Zone 3 distance relays to LE resulting from line outages during hurricane events.

Vulnerability assessment is an effective method for identifying critical components and preventing widespread cascading outages [2]. As

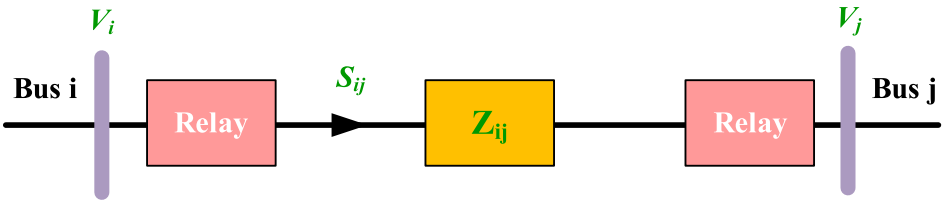

Fig. 5. A transmission line equipped with relays on both ends.

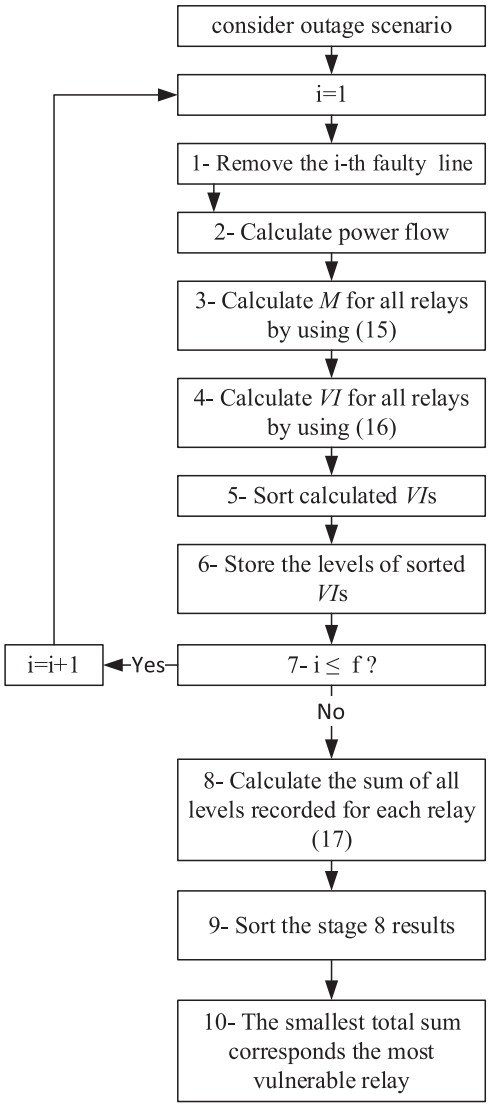

Fig. 6. Scenario-based relay vulnerability assessment.

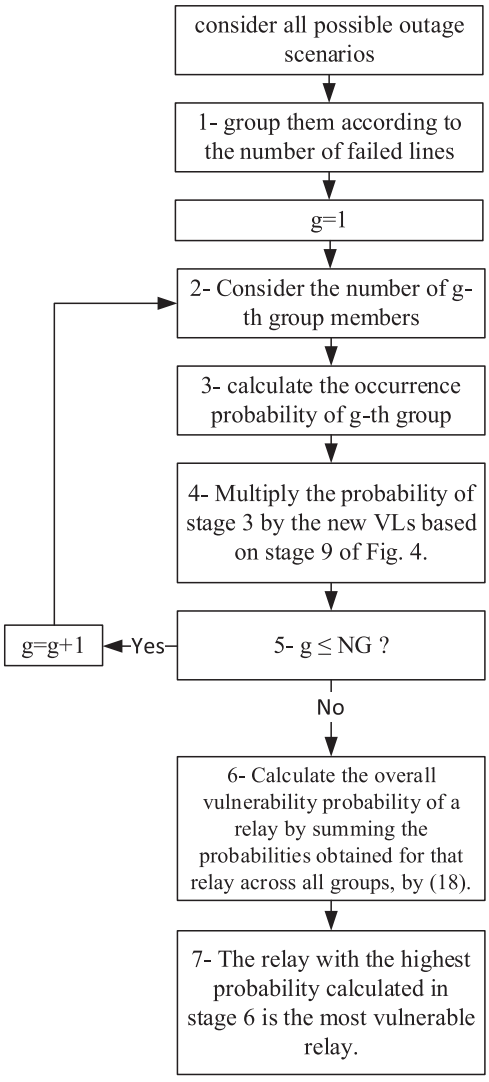

Fig. 7. Relay vulnerability assessment in general.

illustrated in Fig. 1, a resilient system exhibits a lower VL compared to a traditional system. One important factor that can trigger cascading outages is the maloperation of Zone 3 vulnerable distance relays during static LE [23]. The goal of assessing the vulnerability of Zone 3 distance relays is to identify the critical relays that significantly contribute to the propagation of severe cascading outages under various operating conditions [23]. Therefore, the performance of Zone 3 distance relays must be evaluated, and their VLs determined. Fig. 5 depicts a typical transmission line equipped with distance relays at both ends.

The operation margin of a mho distance relay, referred to as the RM, is defined as the difference between the impedance seen by the relay and the Zone-3 setting impedance, as expressed in (15). The Zone 3 setting impedance is assumed to be 2.4 times the impedance of the protected line [46]. If the seen impedance is lower than the Zone 3 setting (i.e., if the value of RM becomes negative), it indicates that the seen impedance has entered the Zone 3 region, leading to tripping of the line. Therefore, according to (15), performance of the Zone 3 distance relay can be evaluated by comparing the measured impedance with the relay's corresponding line impedance setting.

$$RM = Z_{seen} - Z_{set,zone\ 3,\ ij} = Z_{seen} - (2.4 \times Z_{ij}) \quad (15)$$

where RM, Z_{seen}, $Z_{set,\ zone\ 3,\ ij}$, and Z_{ij} are the relay margin, the impedance seen by the distance relay, the setting impedance for Zone 3 of the distance relay and the impedance of the protected line, respectively.

In this paper, a new index based on RM is proposed to evaluate the

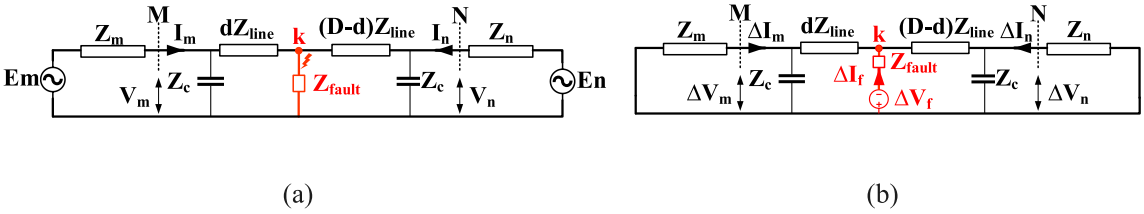

Fig. 8. Transmission network exposed to an in-zone symmetrical fault, (a) single-line diagram and (b) superimposed equivalent circuit.

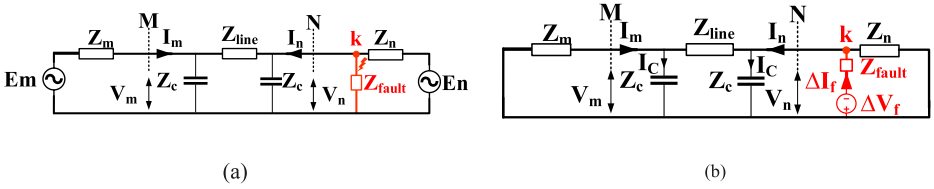

Fig. 9. Transmission network exposed to an out-zone symmetrical fault, (a) single-line diagram and (b) superimposed equivalent circuit.

performance of Zone 3 of the distance relay, as represented in (16).

$$VI = \frac{RM_e - RM_o}{RM_o} \tag{16}$$

where VI, RM_e, and RM_o represent the vulnerability index, RM under event conditions, and RM in normal network operation mode, respectively. Eq. (16) captures the changes in RM compared to steady-state conditions. In other words, RM is calculated for both operation conditions: pre-event and post-event. If the seen impedance is close to Zone 3 of the distance relay, the relay may enter Zone 3, indicating high vulnerability of the distance relay. Therefore, the smaller the index value, the more vulnerable the relay is. Before applying any fault to the transmission network, the RM for the steady state (RM_o) is calculated. Then, the RM after an event (RM_e) is calculated.

Thus, VI can be determined according to (16). In the following, the vulnerability assessment process of distance relays to identify critical relays is conducted based on the proposed VI, considering two viewpoints: (i) vulnerability assessment based on the number of removed lines for a typical scenario, and (ii) vulnerability assessment for all outage scenarios (general case), as illustrated in Figs. 6 and 7, respectively. In both cases, the vulnerability probability of the relays will be calculated. The proposed algorithms are described as follows.

i. **Scenario-based vulnerability assessment**: Scenarios depend on the initial conditions of a hurricane. The algorithm shown in Fig. 6 calculates the vulnerability of relays for a specified hurricane scenario. In this figure, the outage scenario and **f** refer to a failure scenario of transmission lines caused by a hurricane event and the number of failed lines, respectively. The failed lines are disconnected one after another according to their outage sequence, as shown in Fig. 4. According to Fig. 6, after a line outage, the VIs for a transmission network with **Y** relays are calculated. The relays are then ranked based on their VI values, from smallest to largest. In this ranking method, each relay is assigned a value from 1 to **Y**, where the relay with the lowest VI receives a rank of 1, and the relay with the highest VI receives a rank of **Y**. This ranking process is repeated for all line outages, and the VL of each relay is recorded in each iteration. Ultimately, the overall VL for each relay is calculated by summing the recorded ranks of that relay across all line outages, as represented in (17). The relay with the highest overall VL is considered the most vulnerable.

$$VL = \sum_{i=1}^{f} Y_i \tag{17}$$

i. **Vulnerability assessment in general**: By iterating the algorithm of Fig. 6 for various hurricane conditions and generating different scenarios, scenarios whit the same number of failed lines are grouped together. In Fig. 7, **NG** indicates the number of groups. If each group consists of m members and the total number of hurricane scenarios is denoted by S, the probability of occurrence for the g^{th} group can be calculated as m divided by S, i.e., m/S. The sorted relays in each scenario are then re-ranked based on the follows: The relay ranked first is assigned a vulnerability probability of Y/Y, the second-ranked relay receives (Y-1)/Y, and the relay with the lowest ranking is assigned a probability of 1/Y. Next, the rank-based probability of each relay is multiplied by the group probability to determine the PF of that relay within the group. Finally, to obtain the overall vulnerability probabilities of the relays, the "law of total probability" is applied, as represented in (18). This equation calculates the overall vulnerability probability for each relay. Ultimately, the relay with the highest calculated probability is considered the most vulnerable.

$$VP_R = \sum_{i=1}^{NG} OP_{gi} \times FP_{Ri} \tag{18}$$

where VP_R, OP_{gi}, and FP_{Ri} indicate the vulnerability probability of the relay, the occurrence probability of the i^{th} group, and the PF of the relays in the corresponding group.

6. The proposed protection scheme for monitoring the Zone 3 of vulnerable relays

A new MI is proposed to prevent the maloperation of Zone 3 of identified vulnerable distance relays under LE conditions. The proposed index utilizes the SCCP to distinguish between the symmetrical faults located inside the Zone 3 and LE. Since increased line loading and static can initially cause the impedance trajectory to enter Zone 3 of the distance relay— resulting in unnecessary relay operation—, the primary focus of this study is on Zone 3. Hence, Zones 1 and 2 are excluded from the scope of this investigation. Accordingly, the main objective of proposed protection scheme is to monitor the performance of Zone 3 in the identified vulnerable distance relays, with the aim of distinguishing between the symmetrical three-phase faults within the zone and conditions arising from LE. Fig. 8(a) and 9(a) depict the single-line diagram of the equivalent circuit of the protected line by Zone 3 of distance relay located at bus M during in-zone and out-zone symmetrical faults. The

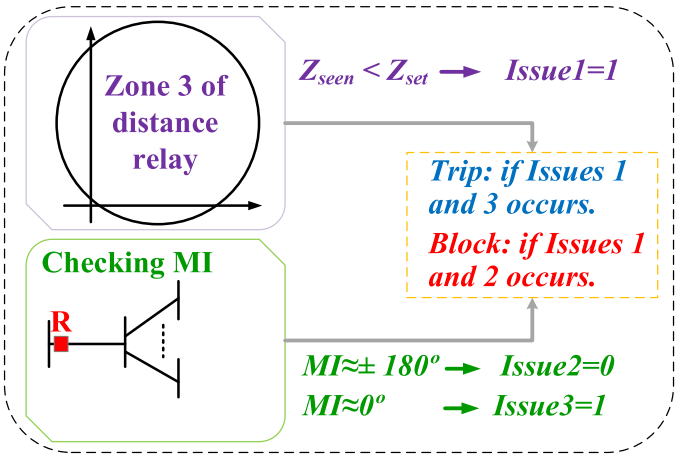

Fig. 10. Control scheme for the correct operation of Zone 3 of the vulnerable distance relay.

fault component superimposed equivalent circuits are illustrated in Fig. 8(b) and 9(b). Let ΔU_m and ΔU_n be the positive-sequence fault component voltage phasors obtained at buses M and N, respectively, while ΔI_m and ΔI_n are the positive-sequence fault component current phasors obtained at the same buses.

The suggested MI, named as 'DPAISCP', is defined as (19):

$$MI_{mn} = \arg(\Delta\overline{S}_m) - \arg(\Delta\overline{S}_n) = \angle\Delta\overline{S}_m - \angle\Delta\overline{S}_n \tag{19}$$

Where, $\Delta\overline{S}_m$ and $\Delta\overline{S}_n$ represent the phasor quantities of SCCP extracted at buses M and N, respectively, which are defined by (20) and (21).

$$\Delta\overline{S}_m = \Delta\overline{V}_m\Delta\overline{I}_m^* \tag{20}$$

$$\Delta\overline{S}_n = \Delta\overline{V}_n\Delta\overline{I}_n^* \tag{21}$$

Under different events, the difference between the SCCP arguments obtained from the two ends of the protected line can help in reliable distinguishing the in-zone symmetrical faults from LE condition. Therefore, the performance of the MI is evaluated under in-zone symmetrical fault conditions, out-zone symmetrical faults and LE conditions.

1. **Symmetrical faults located inside Zone 3:** In Fig. 8(a) the single-line diagram of a power transmission network exposed to an in-zone symmetrical fault at point "k" on the protected line between buses M and N is depicted. The line length between buses M and N, shown in Fig. 8, is set based on the coverage of Zone 3 of the distance relay on bus M. As stated in (15), the Zone 3 reach in this study is assumed to be 2.4 times the length of the protected line. Therefore, symmetrical faults occurring on the MN line are considered as the faults located inside Zone 3.

In Fig. 8, Z_m and Z_n are the Thevenin impedances seen from both sides of the protected line behind the bus M and N. Fig. 8(b) depicts the fault superimposed network during in-zone symmetrical faults. By applying the KVL law and rewriting (20) and (21), the index of MI_{mn} is calculated according to (24).

$$\Delta\overline{S}_m = \Delta\overline{V}_m\Delta\overline{I}_m^* = (-Z_m.\Delta\overline{I}_m).\Delta\overline{I}_m^* = -Z_m.|\Delta I_m|^2 \tag{22}$$

$$\Delta\overline{S}_n = \Delta\overline{V}_n\Delta\overline{I}_n^* = (-Z_n.\Delta\overline{I}_n).\Delta\overline{I}_n^* = -Z_n.|\Delta I_n|^2 \tag{23}$$

$$MI_{mn} = (\angle - Z_m) - (\angle - Z_n) = -\angle Z_m + \angle Z_n \tag{24}$$

In a transmission network, the equivalent source impedance is usually inductive and it is almost equal to X_S. Then the approximate phase angle of equivalent source impedance is close to 90°. Therefore, the amount of MI_{mn} during in-zone faults can be obtained as (25):

$$In-zone faults: \quad MI_{mn} = -\angle jX_m + \angle jX_n \approx 0^\circ \tag{25}$$

Hence, it can be concluded that during an in-zone fault, the MI_{mn} is almost equal to 0°, independent of the fault location and fault resistance.

2. **Symmetrical** faults **located outside Zone 3/ LE condition:** Under out-zone faults or LE conditions, the response of the MI index can be analyzed using the equivalent superimposed network shown in Fig. 9. According to this Figure, the fault/LE location is forward of relay M and backward of relay N. The Zone 3 reach of the distance relay located on bus M is assumed to be equal to the total length of the line between buses M and N. Thereupon, faults outside the MN line are considered as the faults outside Zone 3 (out-zone fault).

In this situation, since the magnitude of the fault current is much larger than that of the line's capacitive charging current, the latter's effect on the fault current is ignored. In high-voltage transmission lines, the inductive reactance significantly outweighs the ohmic resistance, resulting in a high X/R (typically in the range of 10–20 for a 400 kV system). Consequently, the resistive component of the line impedance can be neglected, and the impedance angle approaches 90 degrees. By applying the KVL law at buses M and N in Fig. 9(b), the values of SCCP are obtained as (26) and (27).

$$\Delta\overline{S}_m = \Delta\overline{V}_m\Delta\overline{I}_m^* = (-Z_m.\Delta\overline{I}_m).\Delta\overline{I}_m^* = -Z_m.|\Delta I_m|^2 = -(R_m + j.X_m)|\Delta I_m|^2 \approx -jX_m|\Delta I_m|^2 \tag{26}$$

$$\Delta\overline{S}_n = \Delta\overline{V}_n\Delta\overline{I}_n^* = \left(Z_m + Z_{Line}\right)\Delta\overline{I}_n.\Delta\overline{I}_n^* = \left(Z_m + Z_{Line}\right)|\Delta I_n|^2 = [(R_m + R_{Line}) + j(X_m + X_{Line})].|\Delta I_n|^2 \approx j\left(X_m + X_{Line}\right).|\Delta I_n|^2 \tag{27}$$

In this state, the phase angle of SCCP in (26) and (27) will approach to 90 degrees and the MI_{mn} for out-zone faults is obtained as (28):

$$MI_{mn} = -\angle j.X_m - \angle j.(X_m + X_{Line}) \approx \pm 180^\circ \tag{28}$$

From the above analysis, it can be concluded that the MI index approaches 0° for in-zone symmetrical faults and approaches ±180° for out-zone faults. Similar to out-zone faults, the LE phenomenon also increases the amount of current flowing through the protected line in one direction. Hence, the LE phenomenon can be considered as an external factor that increases the line loading and can be analyzed and modeled similarly to an out-zone symmetrical fault which is shown in Fig. 9 [26]. The key difference is that the current injected from the equivalent superimposed source, modeled at bus **N**, equals to the increased load current. Therefore, the proposed protection scheme for monitoring the performance of Zone 3 vulnerable distance relays can be implemented according to the following steps:

1) Detecting vulnerable relays under hurricane conditions: Based on the hurricane model and the corresponding assessments, the most vulnerable transmission lines under hurricane conditions are identified. Given that the disconnection of a single line can trigger the unintended tripping of additional lines due to the maloperation of Zone 3 distance relays, the relays are ranked according to their vulnerability. This ranking is determined by analyzing the sequence of line outages and evaluating the resulting power redistribution across the network for each tripping scenario. Using (16), the VI of the relays is calculated. Subsequently, the relays are ranked based on (17). Finally, the vulnerability probability of each relay is determined by using (18), incorporating the occurrence probabilities of the groups discussed in the general vulnerability evaluation. This equation quantifies the likelihood of each relay being vulnerable within different identified groups.

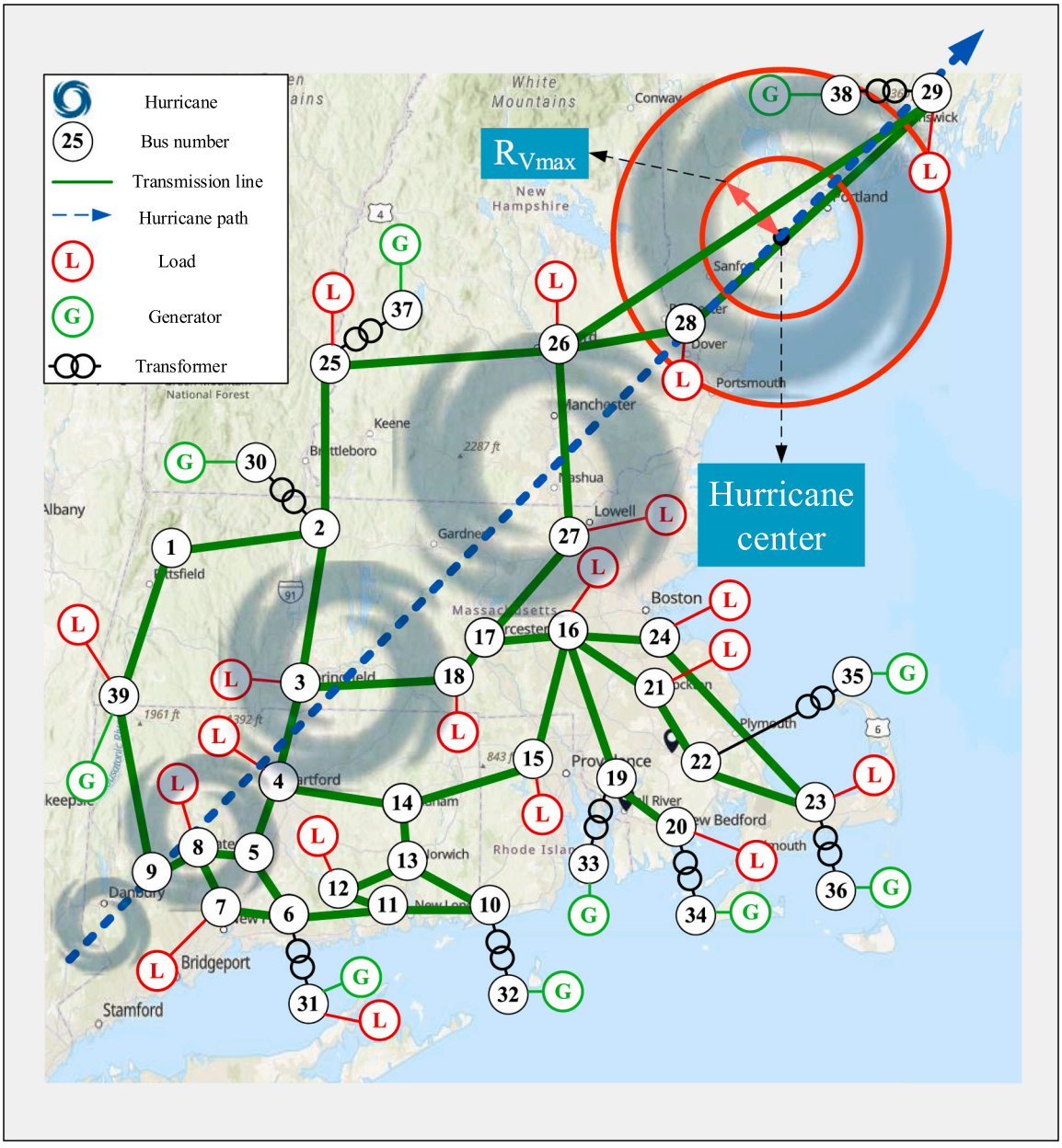

Fig. 11. Configuration of the New England 39 bus test system.

2) Monitoring the performance of Zone 3 of the identified vulnerable relays: Zone 3 of vulnerable distance relays should be monitored to prevent unnecessary operation of distance relays under LE conditions caused by line outages during hurricane. This monitoring will increase the resilience of transmission network during storms. The final criterion for distinguishing the in-zone faults from LE condition is considered as stated by (29) and (30):

$$if: |MI_{mn}| \geq (180^{\circ} \pm \theta^{\circ}) \quad \Rightarrow \text{out} - \text{zoneFault/LE} \ \ is \ \ diagnosed \tag{29}$$

$$if: |MI_{mn}| \leq (0^{\circ} \pm \theta^{\circ}) \quad \Rightarrow in - \text{zoneFault} \ \ is \ \ diagnosed \tag{30}$$

To account for the effects of harmonic distortion, current transformer saturation, measurement errors, and noise on the magnitude of the MI index during in-zone faults or LE conditions, a threshold angle (θ°) is introduced. To enhance the security margin of proposed protection scheme and improve its resilience against the measurement inaccuracies, the threshold angle θ° is set to 60º. This value is determined based on extensive simulations, ensuring effective discrimination between in-zone faults and out-of-zone faults or LE under various conditions. The selected threshold enhances the robustness of the index against variations in fault resistance, fault inception time, and other transient phenomena. Therefore, if the proposed MI index detects an LE condition, the operation of Zone 3 of distance relay should be blocked. Under other fault conditions, the relay can operate according to its settings. In summary, the mechanism for controlling the correct operation of Zone 3 of vulnerable distance relays is illustrated in Fig. 10. By monitoring the performance of Zone 3 of such vulnerable relays during hurricanes, the security and dependability of the transmission network protection scheme are improved, thereby enhancing the resilience of the transmission network.

It is noteworthy that the proposed monitoring scheme in this study is exclusively applied to the identified vulnerable relays, and there is no need to implement a wide-area monitoring system for all relays in the network. However, in order to compute the proposed MI for Zone 3 of vulnerable relays, voltage and current phasors from both ends of the protected line should be known. Hence, the fault component phasor

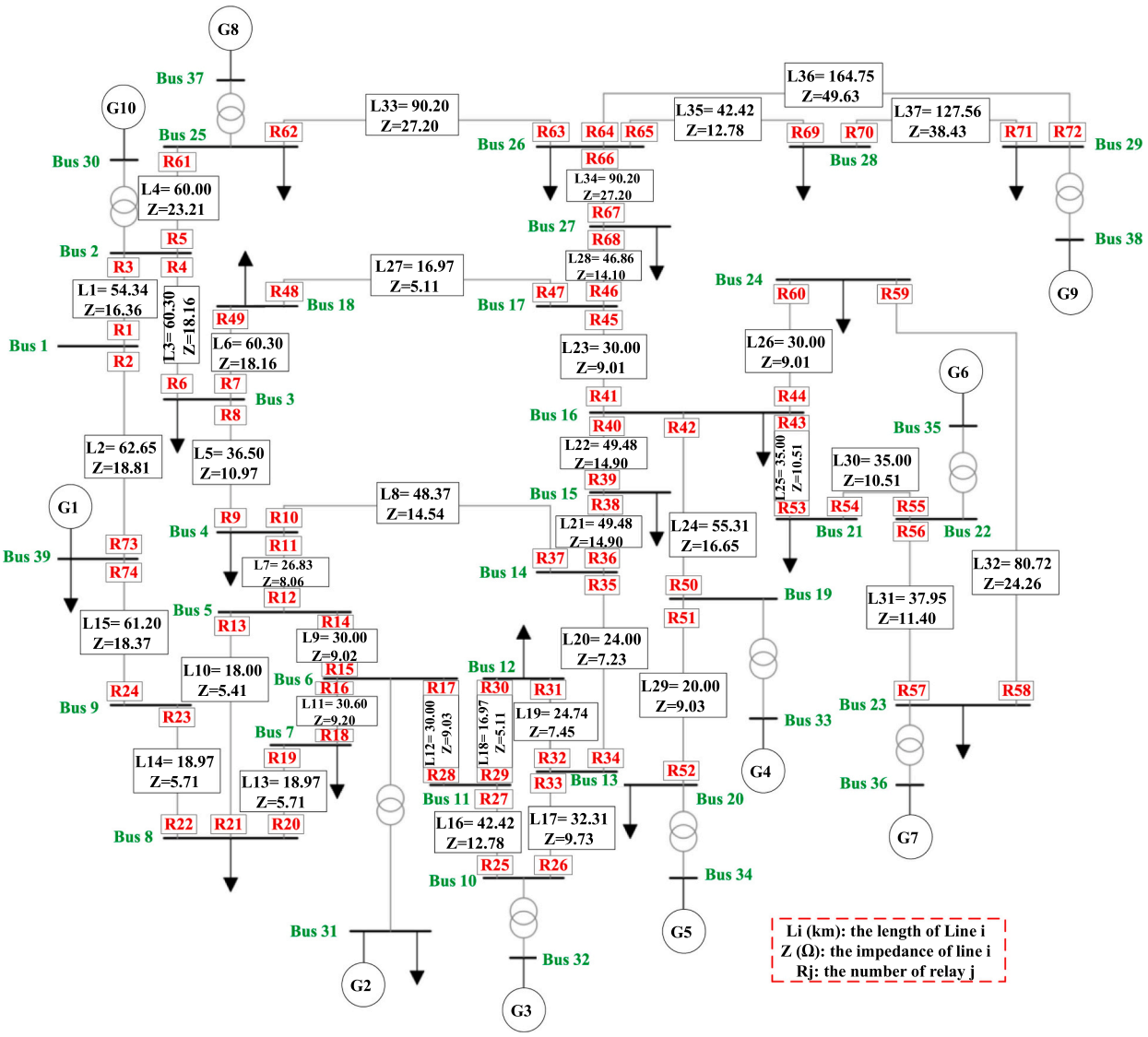

Fig. 12. Specification of the test system.

samples of current and voltage at the remote buses must be acquired using synchrophasor measurement equipment and transmitted to the local bus via a dedicated high-speed communication channel, such as fiber optics. Accordingly, utilizing both the local measurements and received remote data, the MI is computed using (19) to supervise the performance of Zone 3 of vulnerable distance relay protecting that line.

7. Simulation results

7.1. Hurricane model simulation on the test network

To validate the effectiveness of the proposed algorithms and indices, the resilience of the standard 39-bus New England test system under hurricane scenarios is investigated [47]. The geographic layout of the New England transmission network, featuring 39 buses, is illustrated in Fig. 11. The specifications of the test system are shown in Fig. 12, where Li, i, Z, Rj, and j denote the length of the line, line number, impedance of the line, relay, and relay number, respectively. According to [48], the average recorded radius of hurricanes ranges from 6 to 10 km. The hurricane path shown in Fig. 11 is selected based on data from the last 50 years [48]. Based on the hurricane's path, some transmission lines may fail. The disconnected lines and the approximate time of their outages can be estimated using the algorithm presented in Fig. 4 during the hurricane. This method allows identification of cascading outages of transmission lines caused by the hurricane. The number of disconnected lines depends on the initial conditions of the hurricane. Through sensitivity analysis, it is possible to determine which lines will be disconnected at a specific hurricane intensity and time by applying various initial conditions to the algorithm mentioned in Fig. 4.

To generate wind speeds, three key principles are considered:

1. There is a minimum difference of 10 m/s between the wind speeds as the hurricane makes landfall and as it moves away from the land.
2. Incremental changes in wind speeds for creating various scenarios are set at 1 m/s.
3. A hurricane's wind speed is higher when approaching the land compared to when it is moving away.

In this paper, the lines with a PF greater than 0.9 are considered as the candidate lines for outage. The wind speeds used to create the outage scenarios are based on the hurricane categories presented in [13]. Also, the scenarios are arranged according to the descriptions presented in Section 4

The resilience of the test system is evaluated during hurricanes with a constant radius of 9 km and various wind speeds corresponding to different hurricane categories. The results are presented in Table 1. In

Table 1
Cascading outages of transmission lines due to hurricane.

Wind speed (m/s)	10-30	13-30	14-30	19-31	15-32	17-31	22-32	19-33	21-33	22-33	18-34	19-34	28-39	29-41	30-42	22-48	30-63	FT (min)
Number of failed lines	-	-	-	-	-	-	-	-	-	14	14	14	14	14	14	14	14	**31**
	-	-	-	-	-	-	-	15	15	15	15	15	15	15	15	15	15	**55**
	-	-	-	-	-	-	-	-	-	-	-	-	13	13	13	13	13	**61**
	-	-	-	-	-	-	-	-	-	-	-	10	10	10	10	10	10	**76**
	-	-	-	-	-	-	-	-	-	-	-	-	-	-	-	-	11	**82**
	-	-	-	-	-	-	-	-	-	-	-	-	-	-	-	9	9	**122**
	-	-	-	-	-	-	7	7	7	7	7	7	7	7	7	7	7	**124**
	-	-	-	5	5	5	5	5	5	5	5	5	5	5	5	5	5	**185**
	-	-	-	-	-	-	-	-	8	8	8	8	8	8	8	8	8	**209**
	-	6	6	6	6	6	6	6	6	6	6	6	6	6	6	6	6	**289**
	-	-	-	-	-	3	3	3	3	3	3	3	3	3	3	3	3	**309**
	-	-	-	-	-	-	-	-	-	-	-	-	-	-	27	27	27	**374**
	-	-	28	28	28	28	28	28	28	28	28	28	28	28	28	28	28	**446**
	-	-	-	-	-	-	-	-	-	-	-	-	-	23	23	23	23	**468**
	34	34	34	34	34	34	34	34	34	34	34	34	34	34	34	34	34	**564**
	-	-	-	-	35	35	35	35	35	35	35	35	35	35	35	35	35	**656**
	-	-	-	-	-	-	-	-	-	-	33	33	33	33	33	33	33	**657**
	36	36	36	36	36	36	36	36	36	36	36	36	36	36	36	36	36	**810**
	37	37	37	37	37	37	37	37	37	37	37	37	37	37	37	37	37	**836**
Occurrence probability	0.0038	0.0025	0.0195	0.0100	0.0087	0.0100	0.0062	0.0087	0.0025	0.0062	0.0347	0.1427	0.0732	0.0533	0.0943	0.3450s	0.1787	

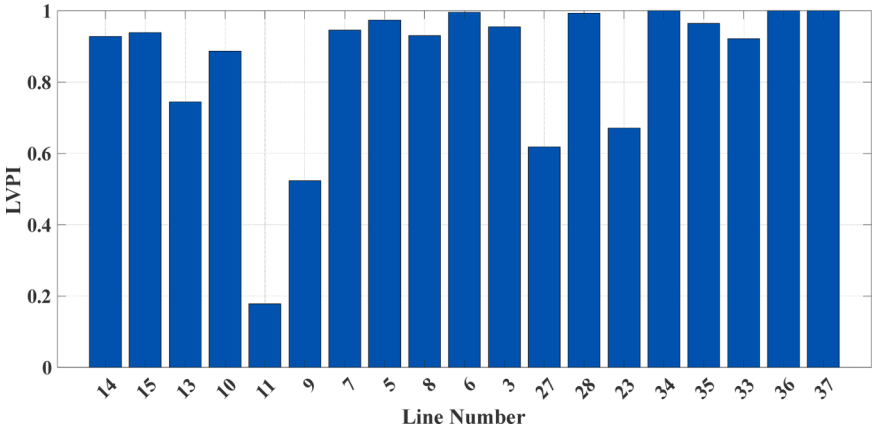

Fig. 13. Vulnerability of lines.

this table, the wind speed shows the speeds when the hurricane is leaving and entering the land, respectively. For example, "10–30" means that the hurricane enters the land with a wind speed of 30 m/s and leaves it with a wind speed of 10 m/s. Moreover, the number of disconnected lines and the occurrence probability in the first column represent the number of failed lines under the hurricane event and the group probability. At the mentioned wind speed, lines 34, 36, and 37 have a PF greater than 0.9 and are considered out of service. It is noteworthy that, due to the numerous scenarios, Table 1 only includes cases where the number of disconnected lines varies with changing wind speed. In other words, this table indicates the lowest wind speed at which a certain number of lines are disconnected. The last row of each

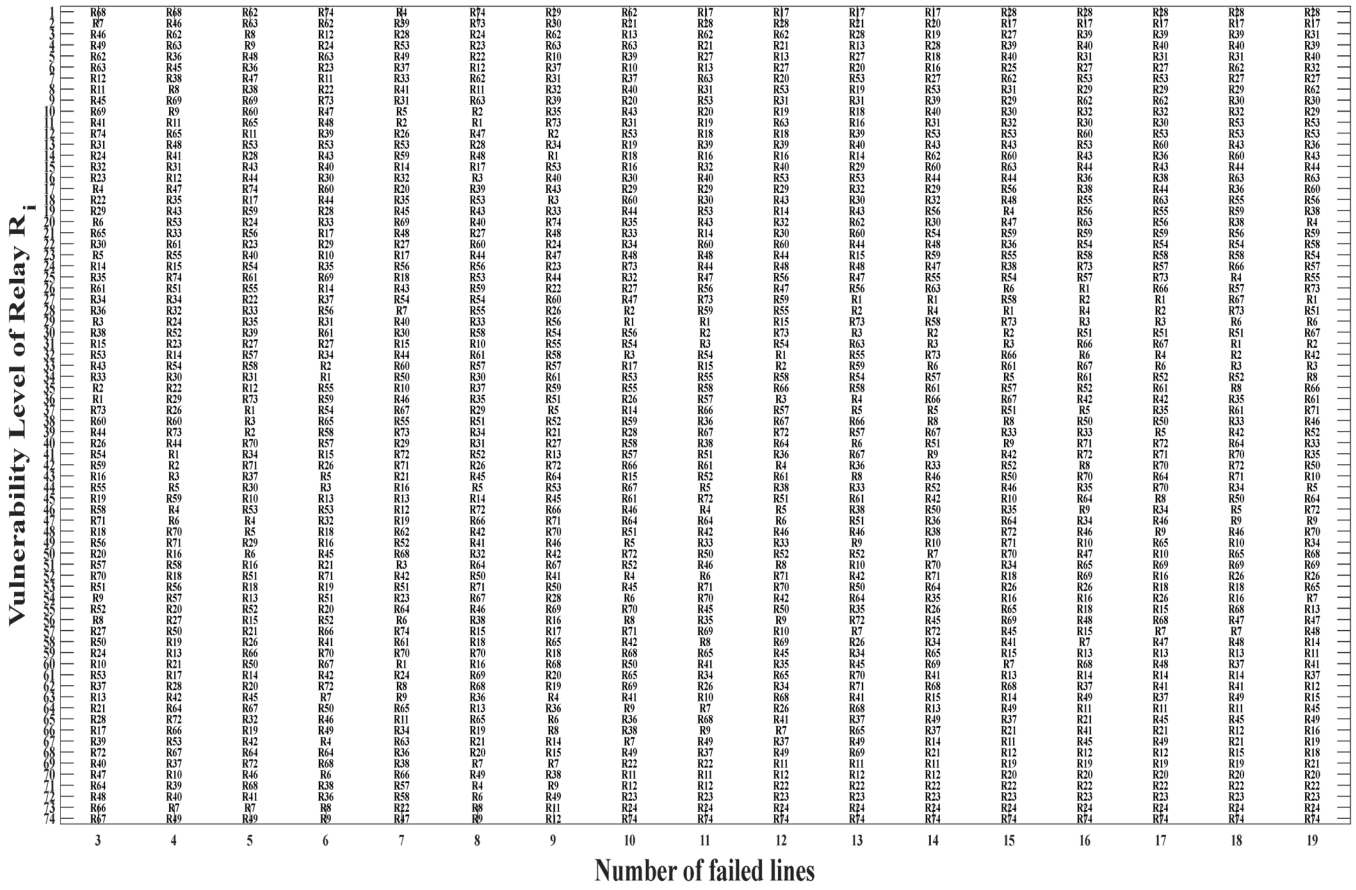

Fig. 14. Ranking the vulnerability of Zone 3 of distance relays from the highest to the lowest in different scenarios.

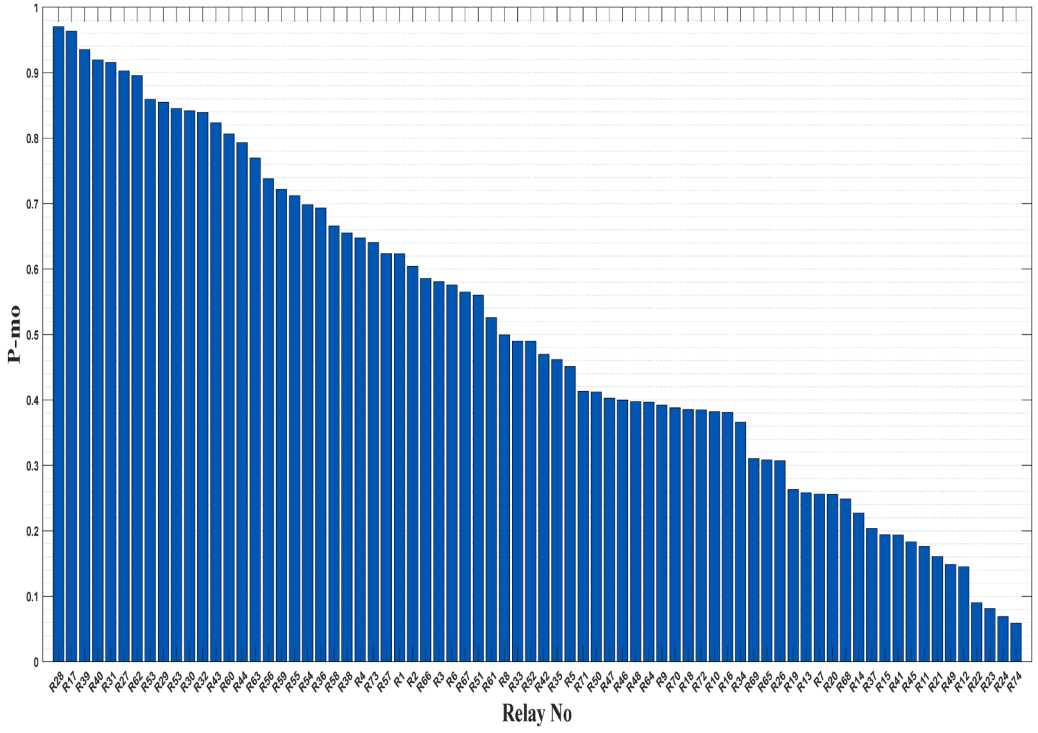

Fig. 15. Vulnerability probability of the relays under hurricane.

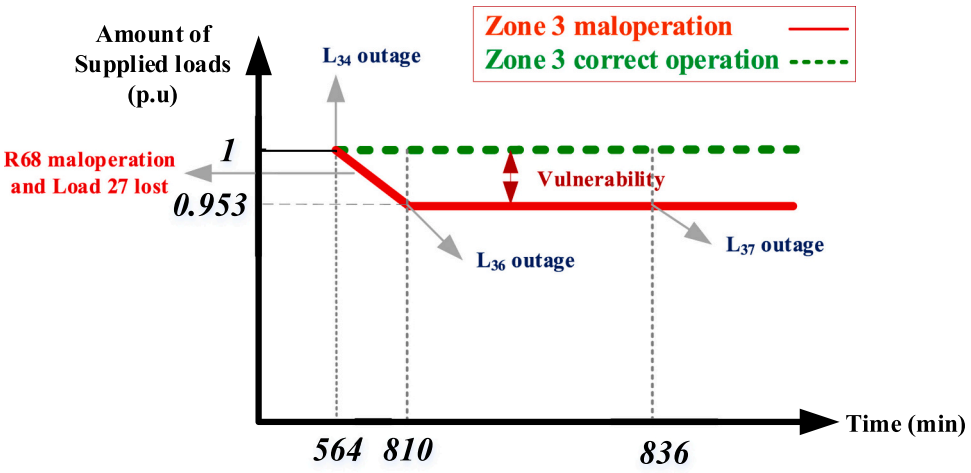

Fig. 16. Resilience curve by considering the maloperation of the distance relay.

Table 2
The most vulnerable relays under IAN hurricane.

line number	14	15	13	10	11
relay No	R9	R9	R21	R28	R17
line number	9	7	5	8	6
relay No	R8	R8	R7	R28	R28
line number	3	27	28	23	34
relay No	R68	R68	R28	R28	R2
line number	35	33	36	37	-
relay No	R2	R28	R28	R28	-

column displays the group occurrence probability. For instance, the outage probability of three lines due to hurricanes scenarios is 0.0038. According to (14), the vulnerability of the test system lines is shown in Fig. 13. The most vulnerable lines are 34, 36, and 37. It is worth noting that the vulnerable lines may change depending on variations in the radius and path of the hurricane.

7.2. Identifying vulnerable Zone 3 of a distance relay

7.2.1. Based on a single scenario

The sequences of the failed lines are determined by the algorithm mentioned in Fig. 4. Then, employing the algorithm presented in Fig. 6 identifies the vulnerable Zone 3 of the distance relays. The results are shown in Fig. 14. For instance, in scenarios with three failed lines, the lines are taken out of service according to the chain $CFC = \{L_{34}, L_{36}, L_{37}\}$. After removing Line 34, a power flow analysis is conducted to obtain the network parameters. Subsequently, all RMs are calculated using (15). Then, the proposed VI is determined for all relays and sorted. The relay with the smallest VI is identified as the most vulnerable relay due to that outage chain.

This process is repeated for the second and third line outages, and the VLs for each relay during these outages are summed to produce a final value. Therefore, the relay with the smallest final value is determined to be the most vulnerable in this specific scenario. This process is applied to other scenarios, and the order of vulnerable relays is determined based on the number and sequence of disconnected lines. The results of the

Table 3
Results of RM and VI after the outage of line 14 under IAN hurricane.

Relay No	**R9**	**R8**	**R21**	**R13**	**R46**	**R6**	**R4**	**R20**
RM	1052.89	1140.70	710.0708106	736.5721982	4967.164584	456.581	471.772	725.07
VI	−0.26094	−0.24147	−0.216149584	−0.188920908	−0.146632741	−0.14398	−0.14326	−0.13468
Relay No	**R19**	**R18**	**R17**	**R28**	**R16**	**R62**	**R39**	**R27**
RM	750.576	373.247	947.2381051	954.9881051	383.5184617	2710.89	548.535	608.594
VI	−0.10689	−0.10204	−0.096476223	−0.091840126	−0.085391854	−0.0804	−0.05917	−0.04544
Relay No	**R40**	**R14**	**R53**	**R43**	**R67**	**R66**	**R33**	**R25**
RM	563.127	711.953	1034.644876	996.4425586	710.5275287	763.654	600.653	627.247
VI	−0.03912	−0.03695	−0.033056711	−0.032588035	−0.026423338	−0.02618	−0.02491	−0.02416
Relay No	**R56**	**R44**	**R60**	**R54**	**R59**	**R55**	**R58**	**R15**
RM	771.824	587.793	606.5149523	406.5716531	324.1134581	430.010	327.298	736.619
VI	−0.02409	−0.02069	−0.020442043	−0.01525309	−0.01503933	−0.01452	−0.01451	−0.01256
Relay No	**R10**	**R37**	**R31**	**R48**	**R47**	**R68**	**R64**	**R63**
RM	425.570	426.424	2039.529372	1444.486756	1446.361756	8738.16	756.494	2499.02
VI	−0.00894	−0.0072	−0.0069882	−0.004222357	−0.00344504	−0.003	−0.00216	−0.00191
Relay No	**R65**	**R70**	**R57**	**R69**	**R51**	**R72**	**R71**	**R52**
RM	2730.87	688.783	743.6898334	2732.942929	102.4572683	762.104	693.196	69.3434
VI	−0.00188	−0.00164	−0.00154687	−0.001461485	−0.00117841	−0.0007	−0.00069	0.00445
Relay No	**R35**	**R34**	**R26**	**R42**	**R50**	**R61**	**R45**	**R30**
RM	463.193	467.999	634.5615731	314.4969037	302.3710533	803.584	1228.58	1577.55
VI	0.00740	0.00783	0.014325927	0.020207058	0.021803761	0.02344	0.03276	0.03852
Relay No	**R29**	**R5**	**R32**	**R41**	**R49**	**R38**	**R36**	**R3**
RM	1662.02	833.273	2037.705842	1176.160878	8696.936304	2262.58	2435.61	1936.24
VI	0.04032	0.05052	0.052681516	0.067630017	0.246294325	0.33332	0.35503	0.39610
Relay No	**R73**	**R1**	**R2**	**R7**	**R12**	**R74**	**R11**	**R24**
RM	1929.028	2056.33	2050.450043	17461.9363	8600.642675	7062.91	11492.3	inf
VI	0.459624	0.48217	0.48421814	0.494034948	1.96823694	3.28561	3.32150	inf

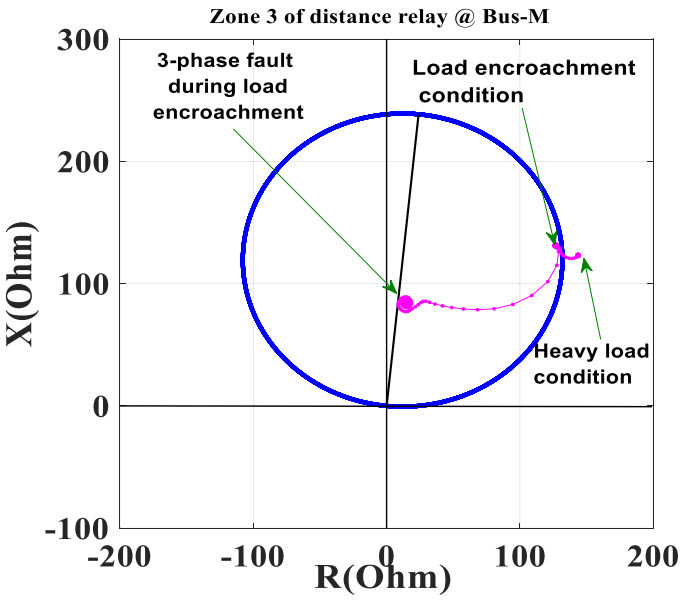

Fig. 17. Trajectory of impedance seen by relay R28 after disconnecting lines of 14, 15, 13, and 10.

vulnerability assessment for various scenarios are presented in Fig. 14, where the relays are ranked from highest to lowest vulnerability. The vertical axis indicates the VL of the relays, with 1 representing the most vulnerable relay and 74 representing the least vulnerable. The horizontal axis represents the number of transmission lines that are out of service due to hurricane occurrence. According to Table 1 and Fig. 14, identifying the VL of the distance relays depends on both the number of line outages and their outage sequence.

7.2.2. *Based on all the scenarios*

The vulnerability assessment of the relays, considering all outage scenarios, is also performed. To this end, the algorithm illustrated in Fig. 7 is utilized. This algorithm categorizes all line outage scenarios based on the number of disconnected lines. The probabilities for each category are calculated and provided in Table 1. Moreover, as mentioned in Section 5, for the relays ranked according to Fig. 14, a value should be assigned between 1 and (1/Y). This procedure determines the PF of the relays based on a group event. This process is repeated for all the scenarios listed in Fig. 14. To derive the PF of each relay, the vulnerability probability of the relay within each group must be multiplied by the group's probability. Finally, the results of these multiplications for each relay are summed to obtain the overall vulnerability probability for that relay. Fig. 15 shows the vulnerability probability of the relays under different hurricane scenarios, using the initial conditions and data mentioned earlier. In Fig. 15, P-mo indicates the maloperation probability of the relay.

It is important to note that these results are based on the assumption of correct operation of Zone 3 of the distance relay. Hence, if maloperation occurs and contributes to a line trip, the cascading outage of transmission lines may spread and change.

7.3. *Transmission system resilience assessment*

Here, it is assumed that the most vulnerable distance relay, identified according to the algorithm shown in Fig. 6, will operate after each line outage caused by a hurricane and trigger the corresponding line trip. This event reduces the resilience of the power system and, after several line outages, may ultimately lead to a blackout.

To assess the resilience of the power system under maloperation of Zone 3 of a vulnerable distance relay, two situations are considered. First, it is assumed that the vulnerable relay trips solely due to the line outage caused by the hurricane. Second, the vulnerable relay is identified by considering a line trip resulting from the maloperation of the Zone 3 distance relay, and its operation is subsequently restricted. The power system resilience curves based on (1) for the two operating modes of the distance relays—maloperation and correct operation of Zone 3—are shown in Fig. 16. The first mode corresponds to maloperation, while the second mode represents correct operation, illustrated in the scenario with three-line outages due to a hurricane.

For the first scenario, the sequence of line outages due to the hurricane is defined as $CFC = \{L_{34}, L_{36}, L_{37}\}$. Initially, line L_{34} trips, which results in relay R68 being identified as the vulnerable relay according to (16). Its maloperation leads to the disconnection of line L_{28}, causing the loss of load at bus 27. Subsequently, lines L_{36} and L_{37} are disconnected. Their outages trigger the maloperation of relays R7 and R46, respectively. However, the operation of these relays solely does not directly result in load loss, unless their maloperation may initiate cascading outages involving additional lines and relays.

In the second scenario, the first failed line is again L_{34}. As in the first scenario, R68 is identified as the most vulnerable relay. The maloperation of R68 causes line L_{28} to trip, resulting in the disconnection of the load connected to bus 27. Following the second hurricane-induced outage (L_{36}), the procedure is repeated, and R52 is identified as the most vulnerable relay. Fortunately, when Line 29 trips due to the maloperation of R52, the system continues to supply all loads. Finally, the last hurricane-induced outage is line L_{37}. In this case, R61 is identified as the most vulnerable relay. Its operation leads to the tripping of line L_4. Nevertheless, the outage of line L_4 due to the maloperation of R61 does not result in any load loss.

It can be concluded that disconnection of certain lines can activate Zone 3 in some relays, potentially leading to line trips and load losses. As shown in Fig. 16, if the power system can withstand Zone 3 maloperations, it becomes more resilient and the amount of lost load can be reduced. Furthermore, power system resilience is further compromised when a relay maloperation causes multiple lines to trip. In this case, the vulnerability of the power grid increases, leading to instability throughout the entire system.

Therefore, a robust MI should be developed to supervise Zone 3 of vulnerable relays, enabling the distinction between LE and faults to reduce the expansion of cascading outages.

7.4. *Evaluation of the proposed MI performance*

In this section, the performance of the proposed MI is investigated to distinguish LE from faults in the 39-bus test system through simulations performed using PSCAD/EMTDC software. The system data are provided in Fig. 12. Two distance relays are assumed to be installed at both ends of each line. Additionally, the reach of Zone 3 is set to be 2.4 times the impedance of the protected line to cover the entire length of the adjacent line. Hurricane IAN, which occurred in 2022 [49], is selected as the test event. The maximum and minimum recorded wind speeds during this event were approximately 70 m/s and 15 m/s, respectively. It is also assumed that the radius and path of the hurricane correspond to those illustrated in Fig. 11.

The hurricane is simulated on the test system, and the failed lines are identified. The number of failed lines is 19, and their outage sequence follows the scenario with 19 failed lines, as outlined in Table 1. The most vulnerable relays during this scenario are identified using the algorithm illustrated in Fig. 6, with the results presented in Table 2. Line 14 is the first to fail due to the hurricane. It is removed, and the RM and then VI are calculated for all relays. According to the results, relay R9 has the lowest VI value and is therefore selected as the most vulnerable relay due to the outage of line 14. This process is repeated for the remaining failed lines, identifying the most vulnerable relay at each stage. The results are provided in Table 3, which indicates that R28 has the highest likelihood of being a vulnerable relay compared to others. According to this table, the contribution probability of R28 in this scenario is 0.42 %.

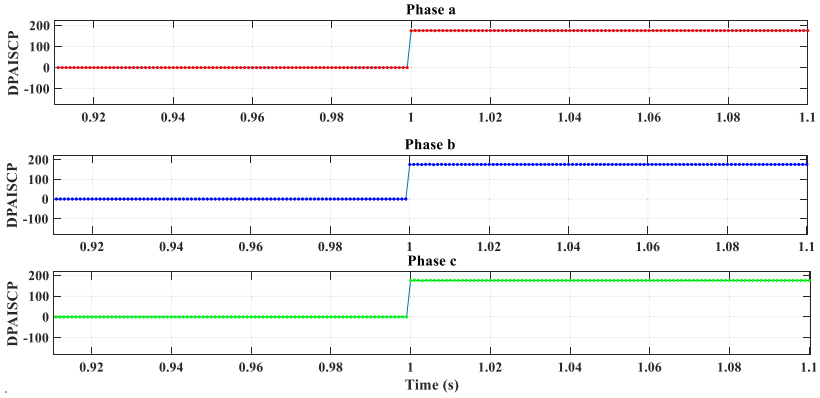

(a)

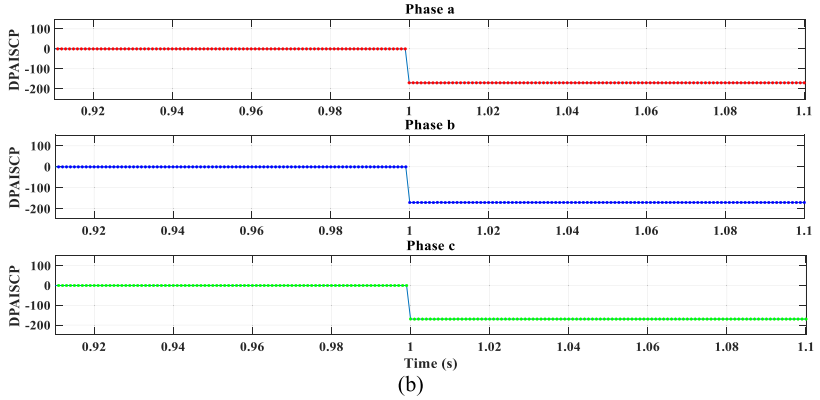

(b)

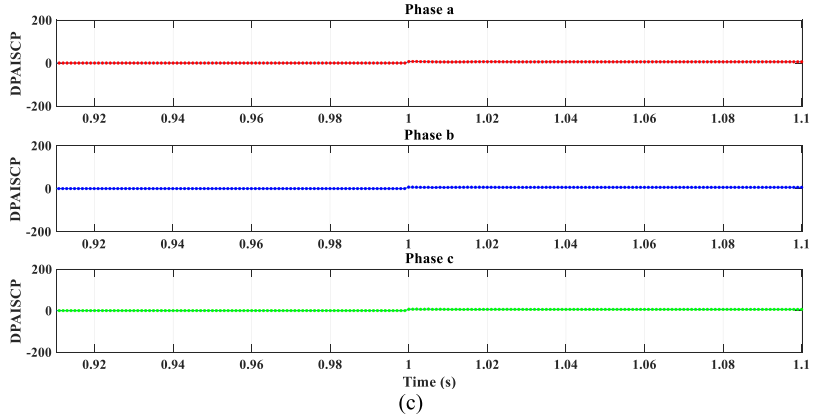

(c)

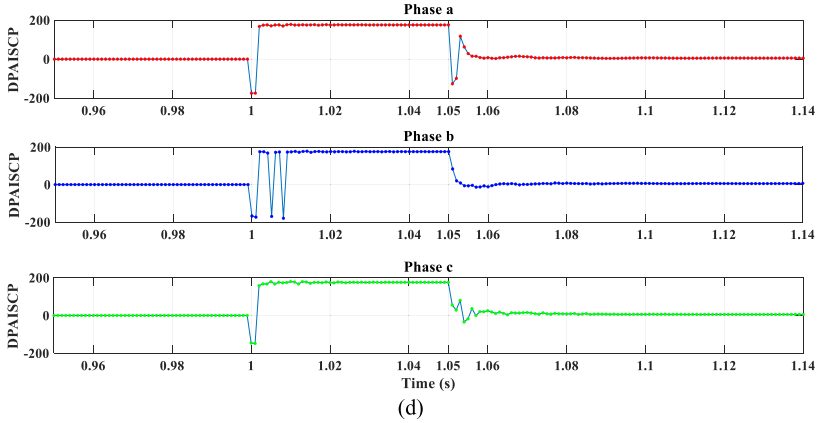

(d)

Fig. 18. Results of the proposed MI (a) under LE, (b) out-zone symmetrical, (c) in-zone symmetrical, and (d) in-zone symmetrical fault conditions.

Table 4
DPAISCP values for different fault resistances for in-zone symmetrical faults.

	Fault Resistance (ohm)	DPAISCPa	DPAISCPb	DPAISCPc
Symmetrical in-zone fault	0	+ 5.07°	+ 5.54°	+ 6.02°
	50	+ 5.73°	+ 5.84°	+ 5.78°
	100	+ 5.75°	+ 5.84°	+ 5.78°
	150	+ 5.75°	+ 5.85°	+ 5.78°
	200	+ 5.76°	+ 5.85°	+ 5.78°
	300	+ 5.76°	+ 5.85°	+ 5.80°
	500	+ 5.79°	+ 5.88°	+ 5.91°
	1000	+ 5.88°	+ 5.99°	+ 6.14°
Symmetrical in-zone LE	0	+ 4.64°	+ 5.11°	+ 5.58°
	50	+ 8.33°	+ 8.44°	+ 8.38°
	100	+ 10.99°	+ 11.09°	+ 11.02°
	150	+ 13.34°	+ 13.45°	+ 13.36°
	200	+ 15.45°	+ 15.57°	+ 15.47°
	300	+ 19.15°	+ 19.29°	+ 19.19°
	500	+ 25.34°	+ 25.53°	+ 25.43°
	1000	+ 38.65°	+ 38.87°	+ 38.85°

%. It means that relay R28 is the most vulnerable relay. This is also shown in Fig. 15. Hence, its operation under fault conditions is selected to evaluate the performance of the MI.

7.4.1. Validation of the MI performance under symmetrical fault condition and LE event

To validate the performance of the proposed MI under different faults, both three-phase symmetrical faults and LE are applied to the test system. LE causes the impedance seen by the relay to decrease. If the seen impedance falls low enough to enter Zone 3 of the distance relay, the relay may make an incorrect decision and trip the line. However, if the relay can successfully distinguish LE from faults, its operation can be blocked during LE conditions. To analyze the performance of the proposed MI in identifying LE, the load on bus 12 is increased. As a result, when line 10 goes out of service, a significant load is transferred onto line 12. This increased load causes the impedance seen by relay R28 to enter Zone 3.

Fig. 17 shows the changes in the impedance seen by R28 during the outages of lines 14, 15, 13, and 10. According to this figure, the loading of line 12 gradually increases with the outages of the aforementioned lines. After line 12 trips, the impedance seen by relay R28 enters Zone 3. The response of the proposed MI during fault and LE conditions is shown in Fig. 18. Based on the analysis in Section 6 for out-zone faults and LE, the MI index should be approximately ±180°. According to Fig. 18(a), at t = 0.98 s, the load increases and the calculated argument for DPAISCP is about 180°. Additionally, a symmetrical three-phase fault is applied to external line 11.

In this case, the calculated MI is approximately −180°, as shown in Fig. 18(b). Therefore, the MI value for out-zone faults and LE approaches ±180°. Finally, a symmetrical three-phase fault is applied to line 12 to assess the dependability of the MI in detecting in-zone faults. As mentioned in Section 6, the MI for in-zone faults should be 0°, which is illustrated in Fig. 18(c). Additionally, to evaluate the MI's reliability in distinguishing between in-zone symmetrical faults and LE, an LE condition is created at t = 1 s, and after 0.05 s, a three-phase symmetrical fault is applied during the LE condition. The response of the MI under this condition is shown in Fig. 18(d). The results indicate that when an LE occurs, the MI index approaches 180°, and when the symmetrical fault occurs at t = 1.05 s, the MI approaches 0°. Therefore, it can be concluded that the proposed MI index performs successfully in reliably distinguishing faults from LE conditions, improving the security and dependability of the transmission network protection scheme. Additionally, during out-zone faults, the DPAISCP calculated for line 12 is close to 180°, whereas its value remains at 0° during in-zone faults. This demonstrates that the proposed MI index can also be applied as a reliable method to distinguish between in-zone and out-zone faults. The results verify the correct performance of the proposed MI. Consequently, implementing the proposed MI allows for effective monitoring of relay performance, reducing relay maloperation and thereby mitigating the spread of cascading outages through appropriate control actions.

7.4.2. Assessing the Effect of High Resistance Fault

In this section, the effectiveness of the proposed MI-based protection scheme is evaluated with varying fault resistance. Fault resistance values of 50, 100, 150, 200, 300, 500, and 1000 ohms are considered. Two scenarios are analyzed: in the first case, a symmetrical in-zone fault is applied, whereas in the second case, a symmetrical in-zone fault is introduced during a LE condition. The simulation results for both scenarios are presented in Table 4. Response of the proposed MI during symmetrical in-zone faults under varying fault resistances are shown in Fig. 19. As evident, for the case of a pure symmetrical in-zone fault, the value of DPAISCP is approximately equal to zero, confirming the presence of an in-zone fault. When the symmetrical in-zone fault occurs an LE, the DPAISCP value slightly increases but remains below the operational threshold defined in (30). This demonstrates the robustness and reliability of proposed protection scheme in accurately distinguishing the symmetrical in-zone faults from LE conditions, even in the presence of high fault resistances.

7.5. Comparison of the proposed approach with existing methods

In this section, the proposed method for improving the resilience of transmission network against cascading outages caused by hurricanes, is compared with existing methods aimed at reducing network vulnerability due to the unintended operation of protective relays. To this end, Table 5 presents a comparative analysis of the proposed approach and other methods based on several key criteria. As evident, the proposed method demonstrates superior performance in terms of comprehensive resilience assessment. Its main advantages include identification of relays vulnerable to LE triggered by cascading outages, detection of transmission lines susceptible to hurricane-induced failures, real-time monitoring of vulnerable relays to distinguish three-phase faults from LE, development of a detailed hurricane model, simulation of sequential line outages caused by hurricanes, and introduction of a resilience assessment index. Such features collectively highlight the strength and innovation of the proposed approach in enhancing transmission network resilience.

8. Discussion

The implementation of a MI for transmission networks relies on a robust telecommunications infrastructure, particularly through wide-area measurement systems that utilize high-speed communication [53]. While these systems enhance network resilience, they are also susceptible to disruptions caused by hurricanes. To mitigate this vulnerability, it is essential to introduce redundancies and alternative communication strategies.

Designing resilient, multi-layered communication architectures that integrate various technologies such as satellite links, cellular networks, and drone-based communication systems can help ensure continuity during adverse conditions. Solutions such as the development of redundant pathways, including dual landfall cable routes and satellite fallbacks to maintain connectivity, have been explored in [53] to enhance the resilience of this infrastructure.

Ultimately, a well-designed telecommunications framework can significantly improve power system monitoring and coordination during extreme weather events, making it a valuable area for future research.

9. Conclusion

In this paper, a new strategy is proposed to improve the resilience of transmission lines against hurricane-induced cascading outages by

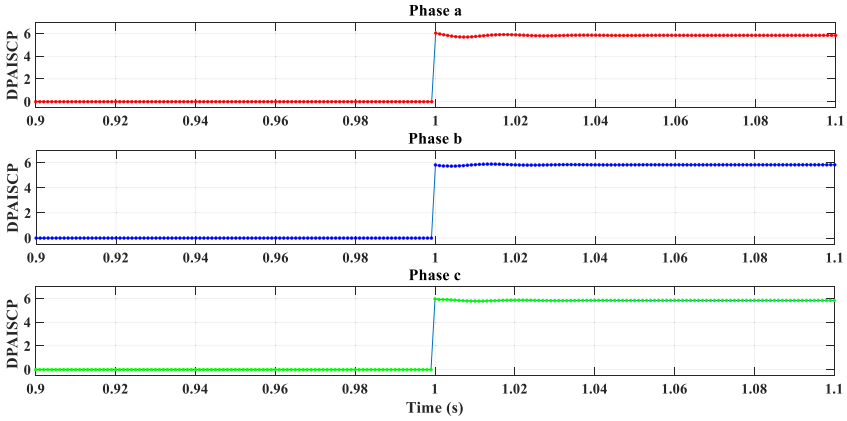

(a)

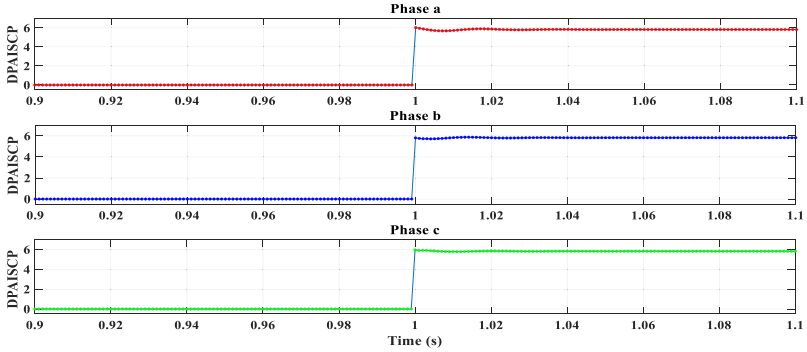

(b)

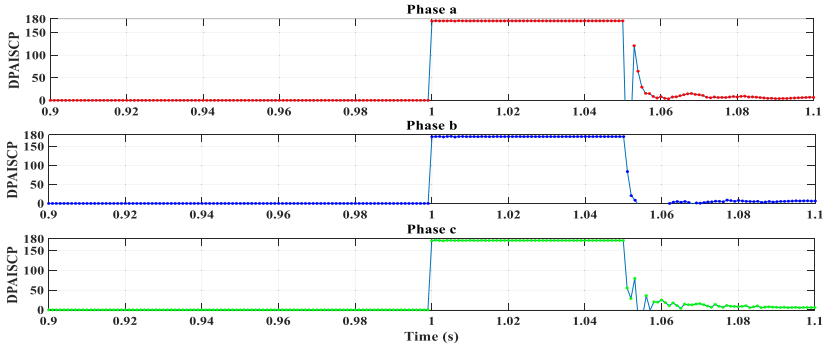

(c)

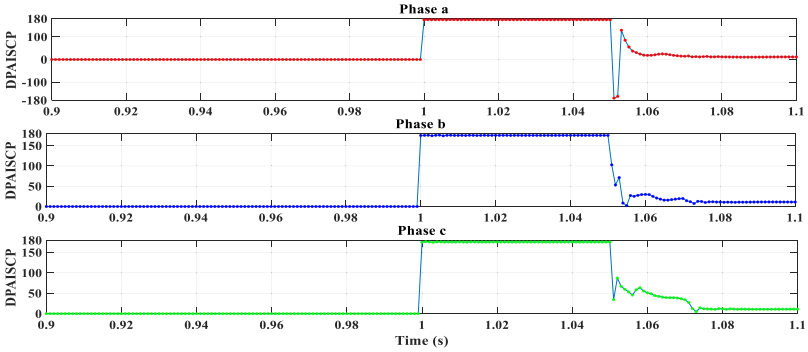

(d)

Fig. 19. Results of the proposed MI during symmetrical, (a): in-zone fault with 50 Ω fault resistance, (b): in-zone fault with 100 Ω fault resistance (c), in-zone fault with 50 Ω fault resistance during LE and, (d) in-zone fault with 100 Ω fault resistance during LE.

Table 5
Comparative Analysis of the Proposed and Previons Methods.

Comparison aspect	[34]	[50]	[30]	[23]	[51]	[28]	[19]	[20]	[10]	[17]	[52]	Proposed method
Vulnerable relay detection	×	×	×	✓	✓	✓	×	×	×	×	×	✓
Vulnerable line detection	×	×	×	×	×	×	✓	✓	✓	✓	✓	✓
Critical relay monitoring	×	×	×	✓	✓	✓	×	×	×	×	×	✓
Symmetrical fault discrimination from LE	✓	✓	✓	✓	✓	✓	×	×	×	×	×	✓
Providing a new hurricane model	×	×	×	×	×	×	×	×	×	×	×	✓
Resilience assessment	×	×	×	×	×	×	×	✓	✓	✓	✓	✓
Line outage sequence modelling due to a hurricane	×	×	×	×	×	×	×	×	×	×	×	✓

preventing the undesired operation of vulnerable Zone 3 distance relays. To achieve this, the vulnerability of transmission lines is investigated using a novel hurricane model, considering the potential maloperation of Zone 3 distance relays. The proposed hurricane model offers two key advantages: it simplifies the complexity of existing models and enhances their accuracy. It is capable of estimating the wind speed at a specific location, determining the hurricane's position at a given time, and predicting the time it will reach a target location. As a result, fragility assessments of power system infrastructure can be performed both accurately and efficiently. Based on this model, the fragility of transmission lines is evaluated, and the sequence of line failures is identified. A new index is introduced to assess the vulnerability of Zone 3 distance relays. Additionally, two algorithms are proposed to evaluate the vulnerability of these relays to hurricane-induced events. These algorithms are applicable to both scenario-based and general-case assessments. Furthermore, after identifying the vulnerable Zone 3 relays that contribute to cascading outages, a new index based on superimposed components is introduced. This index enables distance relays to distinguish in-zone symmetrical faults from LE events, thereby improving protection system performance during extreme weather conditions. One potential limitation of the proposed protection scheme is the reliance of telecommunications system, as it requires remote bus information to calculate the MI. Additionally, the vulnerability of the telecommunications infrastructure to hurricane-induced disruptions could compromise the reliability of the proposed approach. This issue may be addressed by incorporating redundancy measures or exploring alternative communication strategies to improve system robustness under hurricane conditions.

CRediT authorship contribution statement

Seyyed Alireza Modaberi: Writing – original draft, Validation, Software, Methodology, Formal analysis, Conceptualization. **Saeid Ghassem Zadeh:** Project administration, Investigation, Conceptualization. **Sajjad Tohidi:** Supervision, Investigation, Formal analysis. **Tohid Ghanizadeh Bolandi:** Writing – review & editing, Supervision, Project administration, Investigation, Conceptualization.

Declaration of Competing Interest

The authors declare that they have no known competing financial interests or personal relationships that could have appeared to influence the work reported in this paper.

Data availability

No data was used for the research described in the article.

References

[1] S.A. Modaberi, S. Tohidi, S.G. Zadeh, T.G. Bolandi, A review of power system resilience assessment and enhancement approaches by focusing on wind farms and wind turbines, IET Renew. Power Gener. 17 (9) (2023) 2391–2410.

[2] A. Dadashzade, H. Bagherzadeh, M. Mottaghizadeh, T.G. Bolandi, M.H. Amirioun, M. Majidzadeh, et al., Electricity distribution networks resilience in area exposed to salt dust: fragility curve modeling of insulators, monte Carlo-based resilience assessment, and enhancement measures, Heliyon 10 (16) (2024).

[3] K. Shafiei, S.G. Zadeh, M.T. Hagh, Planning for a network system with renewable resources and battery energy storage, focused on enhancing resilience, J. Energy Storage 87 (2024) 111339.

[4] V.S. Tabar, S. Ghassemzadeh, S. Tohidi, Increasing resiliency against information vulnerability of renewable resources in the operation of smart multi-area microgrid, Energy 220 (2021) 119776.

[5] M. Khoshbouy, A. Yazdaninejadi, T.G. Bolandi, Transmission line adaptive protection scheme: a new fault detection approach based on pilot superimposed impedance, Int. J. Electr. Power Energy Syst. 137 (2022) 107826.

[6] A. Kwasinski, F. Andrade, M.J. Castro-Sitiriche, O'Neill-Carrillo E. Hurricane maria effects on Puerto Rico electric power infrastructure, IEEE Power Energy Technol. Syst. J. 6 (1) (2019) 85–94.

[7] A.R. Jordehi, S.A. Mansouri, M. Tostado-Véliz, A. Ahmarinejad, F. Jurado, Resilience-oriented placement of multi-carrier microgrids in power systems with switchable transmission lines, Int. J. Hydrog. Energy 50 (2024) 175–185.

[8] J. Gargani, Impact of major hurricanes on electricity energy production, Int. J. Disaster Risk Reduct. 67 (2022) 102643.

[9] M. Panteli, D.N. Trakas, P. Mancarella, N.D. Hatziargyriou, Boosting the power grid resilience to extreme weather events using defensive islanding, IEEE Trans. Smart Grid 7 (6) (2016) 2913–2922.

[10] J. Zhou, H. Zhang, H. Cheng, S. Zhang, L. Liu, Z. Wang, et al., Resilience-oriented hardening and expansion planning of transmission system under hurricane impact, CSEE J. Power Energy Syst. (2024).

[11] S. Madadi, B. Mohammadi-Ivatloo, S. Tohidi, Integrated transmission expansion and PMU planning considering dynamic thermal rating in uncertain environment, IET Gener. Transm. Distrib. 14 (10) (2020) 1973–1984.

[12] F. Amini, S. Ghassemzadeh, N. Rostami, V.S. Tabar, Electrical energy systems resilience: a comprehensive review on definitions, challenges, enhancements and future proceedings, IET Renew. Power Gener. 17 (7) (2023) 1835–1858.

[13] H. Ranjbar, S.H. Hosseini, H. Zareipour, Resiliency-oriented planning of transmission systems and distributed energy resources, IEEE Trans. Power Syst. 36 (5) (2021) 4114–4125.

[14] J. Winkler, L. Duenas-Osorio, R. Stein, D. Subramanian, Performance assessment of topologically diverse power systems subjected to hurricane events, Reliab. Eng. Syst. Saf. 95 (4) (2010) 323–336.

[15] J. Guo, T. Feng, Z. Cai, X. Lian, W. Tang, Vulnerability assessment for power transmission lines under typhoon weather based on a cascading failure state transition diagram, Energies 13 (14) (2020) 3681.

[16] M. Moradi-Sepahvand, T. Amraee, S.S. Gougheri, Deep learning based hurricane resilient coplanning of transmission lines, battery energy storages, and wind farms, IEEE Trans. Ind. Inform. 18 (3) (2021) 2120–2131.

[17] K. Jalilpoor, A. Oshnoei, B. Mohammadi-Ivatloo, A. Anvari-Moghaddam, Network hardening and optimal placement of microgrids to improve transmission system resilience: a two-stage linear program, Reliab. Eng. Syst. Saf. 224 (2022) 108536.

[18] Y. Yuan, H. Zhang, H. Cheng, Z. Wang, Resilience-oriented transmission expansion planning with optimal transmission switching under typhoon weather, CSEE J. Power Energy Syst. 10 (1) (2022) 129–138.

[19] S.U. Khan, M.S. Khan, H. Farooq, Aggregated vulnerability assessment of power transmission lines under operational and hurricane induced outages, Electr. Power Syst. Res. 240 (2025) 111262.

[20] J. Zhou, H. Zhang, H. Cheng, S. Zhang, Z. Wang, X. Zhang, Resilience-Oriented transmission expansion planning under hurricane impact considering vulnerable line identification and hardening, Prot. Control Mod. Power Syst. 10 (3) (2025) 98–113.

[21] M.S. Parniani, M. Sanaye-Pasand, P. Jafarian, A blocking scheme for enhancement of distance relay security under stressed system conditions, Int. J. Electr. Power Energy Syst. 94 (2018) 104–115.

[22] I. Dobson, Cascading network failure in power grid blackouts. Encyclopedia of Systems and Control, Springer, 2021, pp. 199–202.

[23] T.G. Bolandi, V. Talavat, J. Morsali, Online vulnerability assessment of Zone-3 distance relays against static load encroachment: a novel approach based on fault chain theory, Int. J. Electr. Power Energy Syst. 151 (2023) 109183.

[24] K. Venkatanagaraju, M. Biswal, A.Y. Abdelaziz, Protection system failure and power system blackout. Uncertainties in Modern Power Systems, Elsevier, 2021, pp. 257–296.
[25] M. Arumuga, M.J.B. Reddy, Distance protection methodology for detection of faulted phase and fault along with power swing using apparent impedance, IEEE Access 10 (2022) 43583–43597.
[26] T. Ghanizadeh Bolandi, M.R. Haghifam, M. Khederzadeh, Real-time monitoring of zone 3 vulnerable distance relays to prevent maloperation under load encroachment condition, IET Gener. Transm. Distrib. 11 (8) (2017) 1878–1888.
[27] M.-R.H. Rezaeieh, T.G. Bolandi, S.M. Jalalat, A novel approach for resilient protection of AC microgrid based on differential phase angle of superimposed complex power, Sustain. Energy Grids Netw. 34 (2023) 101024.
[28] T. Ghanizadeh Bolandi, A. Yazdaninejadi, Vulnerability assessment approach for real-time and regional monitoring of backup protections: minimising number of GPS-based distance relays, IET Gener. Transm. Distrib. 14 (14) (2020) 2687–2697.
[29] B. Patel, Superimposed components of lissajous pattern based feature extraction for classification and localization of transmission line faults, Electr. Power Syst. Res. 215 (2023) 109007.
[30] S. Ansari, N. Ghaffarzadeh, A novel superimposed component-based protection method for multi-terminal transmission lines using phaselet transform, IET Gener. Transm. Distrib. 17 (2) (2023) 469–485.
[31] A.M. Joshua, K.P. Vittal, Superimposed current based differential protection scheme for AC microgrid feeders, Appl. Energy 341 (2023) 121079.
[32] S. Ansari, O.H. Gupta, O.P. Malik, Fault detection for microgrid feeders using features based on superimposed positive-sequence power, J. Mod. Power Syst. Clean. Energy 11 (6) (2023) 1948–1958.
[33] K. Dubey, P. Jena, Novel fault detection & classification index for active distribution network using differential components, IEEE Trans. Ind. Appl. (2024).
[34] A. Meidani, M. Abedini, M. Sanaye-Pasand, Enhancing performance of distance relay zone 3 under stressed conditions using an Angle-Based algorithm, IEEE Syst. J. (2025).
[35] S.A. Sedgh, M. Doostizadeh, F. Aminifar, M. Shahidehpour, Resilient-enhancing critical load restoration using mobile power sources with incomplete information, Sustain. Energy Grids Netw. 26 (2021) 100418.
[36] N. Bhusal, M. Abdelmalak, M. Kamruzzaman, M. Benidris, Power system resilience: current practices, challenges, and future directions, Ieee Access 8 (2020) 18064–18086.
[37] G.A. Vecchi, C. Landsea, W. Zhang, G. Villarini, T. Knutson, Changes in atlantic major hurricane frequency since the late-19th century, Nat. Commun. 12 (1) (2021) 4054.
[38] A. Gholami, T. Shekari, F. Aminifar, M. Shahidehpour, Microgrid scheduling with uncertainty: the quest for resilience, IEEE Trans. Smart Grid 7 (6) (2016) 2849–2858.
[39] M. Eliassi, H. Seifi, M.R. Haghifam, Incorporation of protection system failures into bulk power system reliability assessment by Bayesian networks, IET Gener. Transm. Distrib. 9 (11) (2015) 1226–1234.
[40] X. Yu, C. Singh, Probabilistic power system security analysis considering protection failures, COMPEL Int. J. Comput. Math. Electr. Electron. Eng. 23 (1) (2004) 35–47.
[41] S.A. Kaloti, B.H. Chowdhury, Toward reaching a consensus on the concept of power system resilience: definitions, assessment frameworks, and metrics, IEEE Access 11 (2023) 81401–81418.
[42] Z. Li, M. Shahidehpour, F. Aminifar, A. Alabdulwahab, Y. Al-Turki, Networked microgrids for enhancing the power system resilience, Proc. IEEE 105 (7) (2017) 1289–1310.
[43] J.L. Rego, C. Li, On the importance of the forward speed of hurricanes in storm surge forecasting: a numerical study, Geophys. Res. Lett. 36 (7) (2009).
[44] A.C. Phadke, C.D. Martino, K.F. Cheung, S.H. Houston, Modeling of tropical cyclone winds and waves for emergency management, Ocean Eng. 30 (4) (2003) 553–578.
[45] M. Panteli, C. Pickering, S. Wilkinson, R. Dawson, P. Mancarella, Power system resilience to extreme weather: fragility modeling, probabilistic impact assessment, and adaptation measures, IEEE Trans. Power Syst. 32 (5) (2016) 3747–3757.
[46] J. Khodaparast, M. Khederzadeh, Three-phase fault detection during power swing by transient monitor, IEEE Trans. Power Syst. 30 (5) (2014) 2558–2565.
[47] Q. Zhang, F. Li, X. Fang, J. Zhao, Implications of electricity and gas price coupling in US new england region, Iscience 27 (1) (2024).
[48] ⟨www.noaa.gov⟩.
[49] ⟨https://www.nhc.noaa.gov/data/tcr/AL092022_Ian.pdf⟩.
[50] U. Mukundarajan, K.S. Swarup, Maloperation of zone-3 distance relay prevention using distribution entropy, IEEE Access (2024).
[51] B. Sahoo, S.R. Samantaray, I. Kamwa, Supervising vulnerable third zone distance relay to enhance wide-area back-up protection systems, IEEE Access 10 (2022) 49862–49872.
[52] L. Ma, V. Christou, P. Bocchini, Framework for probabilistic simulation of power transmission network performance under hurricanes, Reliab. Eng. Syst. Saf. 217 (2022) 108072.
[53] Q. Wang, W. Li, Z. Yu, Q. Abbasi, M. Imran, S. Ansari, et al., An overview of emergency communication networks, Remote Sens. 15 (6) (2023) 1595.